Original Article | Omics Sciences

Correlation of fecal microbiome dysregulation to synovial transcriptome in an equine model of obesity associated osteoarthritis

Lyndah Chow[#^], Gabriella Kawahisa-Piquini[#], Luke Bass, Dean Hendrickson, Ashana Patel, Meagan Rockow, Steven Dow^, Lynn M. Pezzanite^

Department of Clinical Sciences, College of Veterinary Medicine and Biomedical Sciences, Colorado State University, Fort Collins, CO, USA

Contributions: (I) Conception and design: LM Pezzanite, S Dow; (II) Administrative support: LM Pezzanite, L Chow, S Dow; (III) Provision of study materials or patients: L Bass, D Hendrickson, LM Pezzanite, G Kawahisa-Piquini, A Patel, M Rockow; (IV) Collection and assembly of data: L Bass, D Hendrickson, LM Pezzanite, G Kawahisa-Piquini, A Patel, M Rockow; (V) Data analysis and interpretation: L Chow, LM Pezzanite, S Dow; (VI) Manuscript writing: All authors; (VII) Final approval of manuscript: All authors.

[#]These authors contributed equally to this work.

Correspondence to: Lynn M. Pezzanite, DVM, PhD. Department of Clinical Sciences, College of Veterinary Medicine and Biomedical Sciences, Colorado State University, FCampus Delivery 1678, ort Collins, CO 80523, USA. Email: lynn.pezzanite@colostate.edu.

Background: Osteoarthritis (OA) is increasingly thought to be a multifactorial disease in which sustained gut inflammation serves as a continued source of inflammatory mediators driving degenerative processes at distant sites such as joints. The objective of this study was to use the equine model of naturally occurring obesity associated OA to compare the fecal microbiome in OA and health and correlate those findings to differential gene expression synovial fluid (SF) cells, circulating leukocytes and cytokine levels (plasma, SF) towards improved understanding of the interplay between microbiome and immune transcriptome in OA pathophysiology.

Methods: Feces, peripheral blood mononuclear cells (PBMCs), and SF cells were isolated from healthy skeletally mature horses (n=12; 6 males, 6 females) and those with OA (n=6, 2 females, 4 males). Horses were determined to have OA via lameness evaluation, response to intra-articular (IA) diagnostic analgesia, and radiographic and arthroscopic evidence. Horses were excluded who had received medications or joint injections within 2 months. Cytokine analyses of plasma and SF were performed via multiplex immunoassay. Fecal bacterial microbial 16s DNA sequencing was performed and correlated to bulk RNA sequencing of SF cells and PBMC performed using an Illumina based platform.

Results: Horses with OA had higher body condition scores (P=0.009). Cytokines were elevated in plasma [interleukin (IL)-2, IL-6, IL-18, interferon gamma (IFN-γ), interferon gamma inducible protein 10 (CXCL10 or IP-10), granulocyte colony-stimulating factor (G-CSF)] and SF (IL-1β, IL-6, IL-17A, IL-18, IP-10, G-CSF) in OA. Microbial principal coordinate analysis (PCoA) using Bray-Curtis dissimilarity for β-diversity demonstrated distinct grouping of samples from OA versus healthy horses (P=0.003). Faith alpha diversity was reduced in OA (P=0.02). Analysis of microbiome composition showed differential relative abundance of taxa on multiple levels in OA. Specific phyla (*Firmicutes*, *Verrucomicrobia*, *Tenericutes*, *Fibrobacteres*), correlated to transcriptomic differences related to cell structure, extracellular matrix, collagen, laminin, migration, and motility, or immune response to inflammation in OA.

Conclusions: These findings provide compelling evidence for a link between obesity, gut microbiome dysbiosis and differential gene expression in distant joint sites associated with development of OA in a relevant large animal model, establishing a connection here that provides a platform from which development of therapeutic interventions targeting the gut microbiome can build.

^ ORCID: Lyndah Chow, 0000-0002-6413-9517; Steven Dow, 0000-0001-5488-9464; Lynn M. Pezzanite, 0000-0003-4990-5006.

Keywords: Osteoarthritis (OA); microbiome; transcriptome; translational; equine model

Submitted May 31, 2024. Accepted for publication Sep 26, 2024. Published online Dec 13, 2024.
doi: 10.21037/atm-24-109
View this article at: https://dx.doi.org/10.21037/atm-24-109

Introduction

Osteoarthritis (OA) is a painful condition and major source of disability, affecting 655 million people worldwide (1,2). As 66% of patients with OA are overweight, the need to understand possible connections between obesity and how it accelerates OA is paramount (3). Similarly, OA represents one of the most common conditions treated by equine practitioners with a high prevalence in aged populations, affecting up to 80% of horses over fifteen years of age (4).

Highlight box

Key findings

- This work provides key insights into the composition of fecal microbiome dysregulation and transcriptome of synovial fluid and circulating leukocyte cells in health and osteoarthritis (OA), indicating specific bacterial phyla correlate to differential gene expression associated with innate immune alteration in disease.

What is known and what is new?

- Osteoarthritis is a painful condition and major source of disability. Current treatments are palliative, highlighting the need for an improved understanding of OA pathogenesis to facilitate the development of disease-modifying interventions. Dysregulation of the gut microbiome has a profound influence on systemic inflammation and chronic musculoskeletal disease such as OA.
- Here we applied transcriptomic and microbiomic sequencing techniques in a naturally-occurring equine model of obesity-associated OA to define how the cellular and microbial composition within synovial fluid, peripheral blood mononuclear cells and feces are altered and correlated in the presence of OA.

What is the implication, and what should change now?

- These findings provide compelling evidence for a link between obesity, gut microbiome dysbiosis and development of naturally-occurring obesity-associated OA in horses, establishing a connection here to further investigate disease modifying therapies. These findings highlight the potential role of specific bacterial phyla (*Firmicutes*, *Verrucomicrobia*, *Tenericutes*, *Fibrobacteres*), whose overrepresentation correlated to transcriptomic differences related to cell structure, extracellular matrix, collagen, laminin, migration, and motility, or immune response to inflammation in OA. Future studies will seek to define mechanistically the pathogenic roles of key microbial species and their interactions with innate immune cells towards disease-modifying interventions in the OA of obesity.

Obesity is further considered a risk factor for OA in horses as in multiple other species (5-7) which was attributed in the past to increased body weight exerting greater strain on weight-bearing joints (8) and has more recently been recognized to be due to increased adiposity producing inflammatory cytokines contributing to cartilage degradation (9). Increased body condition in horses was further shown to be positively correlated to levels of pro-inflammatory biomarker prostaglandin E2 (PGE2) in plasma (10). The prevalence of obesity in riding horses has been estimated at 20% to 45% (11,12) representing a significant detriment to health as in humans and other companion animals due to development of insulin resistance (13).

The systemic inflammation driving obesity-associated OA has been associated with gut microbiome dysbiosis, proposed to result in a downstream inflammatory signature culminating in macrophage migration to the synovium of the joint and accelerating knee OA in obese individuals (7). Chronic inflammation is commonly seen in obesity in humans, with an increase in pro-inflammatory cytokines such as tumor necrosis factor-α (TNF-α), monocyte chemoattractant protein 1 (MCP-1) and interleukin (IL)-1β driving this inflammatory phenotype (7). Ablation of CCL2 and TNF-α in laboratory species results in protection from OA development without decreasing body weight, further supporting the concept that a decrease in systemic inflammation is protective in the OA of obesity (14,15). Concurrently, detection of bacterial DNA in intra-articular (IA) tissues and gut dysbiosis have been repeatedly linked to progressive OA (16,17). The low-grade sustained systemic inflammation noted in obese and aging populations with OA has been associated with endotoxin translocation from the GI tract to circulation, resulting in elevated lipopolysaccharide (LPS) levels which has been proposed as one possible mechanism to initiate synovial macrophage activation, although the direct link between dysbiosis of the gut microbiome and local joint disease progression in OA has not been fully elucidated (16,18-21).

Studies demonstrating correlations between serum levels of bacterial metabolites and joint degeneration first indicated a link between gut microbiome dysbiosis with OA,

and that microbial communities could further be altered by diet, germ-free environments, and antibiotics towards the goal of maintaining or managing joint homeostasis and OA (22). Additionally, work in laboratory species has demonstrated the potential to manipulate the microbiome towards mitigating joint degeneration in OA (7). However, there is a paucity of available literature in large animal models on mechanisms of obesity-related lameness and furthermore the potential for therapeutic management of OA in the form of dietary supplementation with joint-protective nutraceuticals that exert their action via shifts in native microbiome. The spontaneously occurring model of OA in horses is a particularly valuable model for human OA due to similarities in cartilage thickness, joint volume allowing large sample collection sizes, articular cartilage loading, and disease prevalence compared to other model species (23-26). Taken together, studies to date suggest that the correlation between the net inflammatory effects of increased adiposity (evidenced by increased body mass index or 'body condition score' in veterinary species) (27), microbiome dysregulation, and degenerative joint disease warrants further investigation.

Therefore, the objectives of this study were to compare fecal microbiome from horses with and without OA and to correlate that to the transcriptome of synovial fluid (SF) and peripheral blood mononuclear cells (PBMCs) and cytokine levels in joints and circulation from the same horses. These studies address the overall hypothesis that individuals with OA have a unique gut dysbiosis and inflammasome signature that can be identified by sequencing the gut microbiome and immunome. Key findings were that fecal microbial diversity was reduced in horses with OA and analysis of microbiome composition showed differential relative abundance of taxa on multiple levels. The presence of specific bacterial phyla (*Firmicutes*, *Verrucomicrobia*, *Tenericutes*, *Fibrobacteres*), correlated to transcriptomic differences related to cell structure, extracellular matrix, collagen, laminin, migration, and motility, or the immune response to inflammation in OA. This work builds upon a paradigm shift in the approach to understanding the pathogenesis of OA, from a historically joint-centric model to a new model that focuses on the critical role of microbial dysregulation and systemic inflammation as key driving factors in OA development and progression using the relevant naturally occurring large animal model of equine OA. We present this article in accordance with the ARRIVE reporting checklist (available at https://atm.amegroups.com/article/view/10.21037/atm-24-109/rc).

Methods

Study overview and horse enrollment

Client-owned horses presenting to the Colorado State University Veterinary Teaching Hospital Surgery Service were convenience sampled and enrolled as OA cases. Control horses were university-owned research horses screened for OA as described below. The Institutional Animal Care and Use Committee and Clinical Review Board at Colorado State University approved these studies for SF, blood, and feces sample collection (CSU IACUC exemption and Clinical Review Board approval # 3375 to obtain samples from client-owned horses with OA undergoing arthroscopy; CSU IACUC #1714 to obtain samples from healthy research horses as controls). Methods were conducted according to NIH Guidelines for the Care and Use of Laboratory Animals (8th edition) and national guidelines under which the institution operates.

Horses that were identified to be free of lameness and lacking tarsal synovial effusion or radiographic evidence of tarsal OA (four-view) were enrolled as controls as previously described (28-31). Diagnosis of OA was determined by a combination of clinical lameness, musculoskeletal palpation, improvement of lameness following injection of intrasynovial local anesthetic solution, radiographic evidence of OA and/or macroscopic arthroscopic visualization of cartilage lesions or synovial inflammation (32). Horses were excluded if they had received oral medications (e.g., nonsteroidal anti-inflammatories, antibiotics, anthelmintics) or intrasynovial injections (e.g., local anesthetics, corticosteroids, orthobiologics) within the past two months. Horses had been fed a consistent diet of grass hay at the time of sample collection for a minimum of two months, which was performed non-fasted. Metadata collected from each horse included signalment, body condition score, joint(s) affected, and documentation of radiographic and arthroscopic evidence of OA. Body condition score for horses was graded on a 1 to 9 scale by two observers experienced in the scoring system (diplomates of the American College of Veterinary Surgeons or American Board of Veterinary Practitioners) and averaged to determine the final score as previously described (27). Study overview is summarized in *Figure 1*. As horses were enrolled based on inclusion/exclusion criteria for OA diagnosis and not assigned to receive treatment allocation, randomization of experimental units (i.e., horses) or blinding of investigators was not performed. Additionally, as treatments were not administered, confounders (e.g., order in which treatments were administered) were not

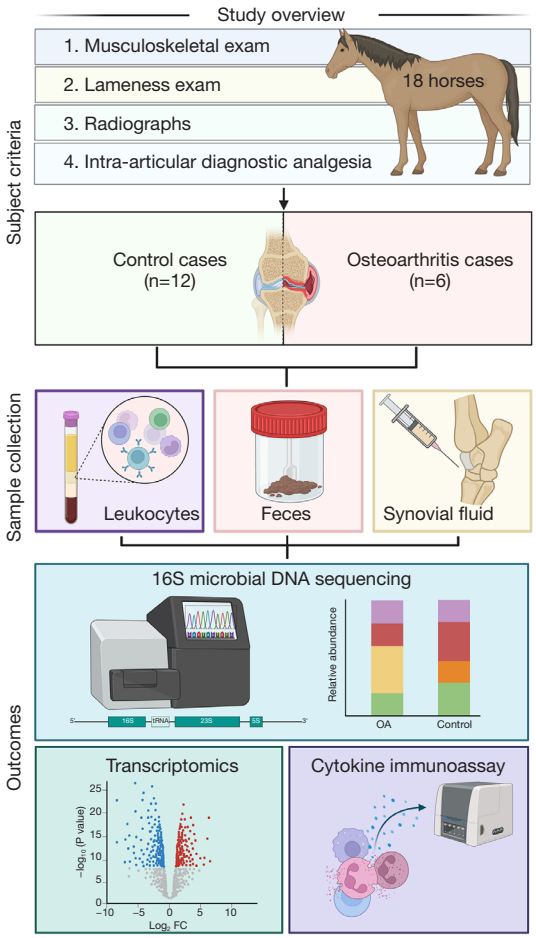

Figure 1 Schematic overview of study design. Horses (n=18) were screened for OA via musculoskeletal examination, lameness evaluation, radiographic evidence of osteoarthritis and improvement in lameness following intra-articular diagnostic analgesia of the affected joint. Horses that received medications including nonsteroidal anti-inflammatories, antibiotics, or anthelmintics or intrasynovial injections or local anesthetic blocking within the two weeks prior to presentation were excluded. Six horses with OA and twelve horses without OA were identified. Synovial fluid (3 to 10 mL) and peripheral blood (20 mL) was obtained from each horse. SF cells were isolated from SF via centrifugation and PBMCs were isolated via Ficoll density centrifugation. RNA was extracted from synovial cells and PBMC using the RNAeasy kit (Qiagen, Germantown, MD, USA) and sent to Novogene Corporation Inc. (Sacramento, CA, USA) for bulk RNA sequencing. RNA quality was determined by bioanalyzer (Agilent Technologies, Santa Clara, CA, USA). mRNA was enriched using oligo (dT) beads, followed by cDNA library generation using TruSeq RNA Library Prep Kit (Illumina, San Diego, CA, USA). Sequencing was performed on Illumina Novaseq 6000 machine using 150 bp paired end reads. Fecal DNA was extracted using a commercially available kit (Qiagen PowerSoil Pro kit) according to manufacturer's instructions. Microbial DNA was frozen at –80 ℃ and sent to ACME at University of Colorado Anschutz Medical Campus, Aurora, CO for microbial sequencing. Samples were run on Illumina Miseq sequencing instruments. Synovial fluid and plasma were aliquoted and stored at –80 ℃. Fluorescent bead-based multiplex assay (Milliplex MAP Equine Cytokine/Chemokine Magnetic Beads Multiplex Assay, Millipore Sigma, Burlington, MA, 01803) was used to quantify the concentrations of 23 analytes [Eotaxin/CCL11, FGF-2, Fractalkine/CS3CL1, G-CSF, GM-CSF, GRO, IFN, IL-1α, IL-1β, IL-2, IL-4, IL-5, IL-6, IL-8/CXCL8, IL-10, IL-12 (p70), IL-13, IL-17a, IL-18, IP-10, MCP-1, RANTES/CCL5 and TNFα] in synovial fluid and plasma aliquots (Figure created using BioRender, courtesy of Zoe Williams). OA, osteoarthritis; SF, synovial fluid; PBMC, peripheral blood mononuclear cell; ACME, Anschutz Center for Microbiome Excellence; G-CSF, granulocyte colony-stimulating factor; GM-CSF, granulocyte-macrophage colony-stimulating factor; GRO, growth related protein; IFN, interferon; IL, interleukin; IP-10, interferon gamma inducible protein 10; MCP-1, monocyte chemoattractant protein-1; TNF-α, tumor necrosis factor-α.

controlled.

Microbiome sample collection and processing

Fresh fecal samples were collected via rectal palpation from the mid-rectum from each horse and placed immediately on ice for not more than one hour for transport to the lab. Fecal samples were aliquoted using aseptic technique into cryovials, flash frozen in liquid nitrogen and stored at –80 ℃. Frozen fecal samples were thawed on ice and DNA extracted using a commercially available kit (Qiagen PowerSoil Pro kit) according to manufacturer's instructions. The quantity and purity of DNA were assessed using a NanoDrop One spectrophotometer (ThermoScientific, Waltham, MA, USA), and samples stored at –80 ℃ until sequencing.

Transcriptomic sample collection and processing

SF samples were obtained in an aseptic environment (e.g., examination room for control horses or surgical suite for OA cases). In OA cases, joints were clipped, aseptically prepared with chlorhexidine and alcohol, and draped in routine fashion, then synoviocentesis was performed of the affected joint immediately prior to distending the joint with crystalloid fluids to perform arthroscopy. In control cases, horses were sedated with a combination of detomidine (0.01 mg/kg IV) and butorphanol (0.01 mg/kg IV) and the tibiotarsal joint was aseptically prepared with chlorhexidine and alcohol for synoviocentesis. To obtain SF samples, a 20-gauge 1.5-inch needle and a 12-mL syringe were used in all cases. SF samples were transported to the laboratory on ice for processing. To isolate synovial cells for sequencing, SF samples were digested with hyaluronidase (30 µg/mL) and incubated at 37 ℃ for 15 minutes, then centrifuged at 2,000 rpm at 8 ℃ for 10 minutes to obtain a cell pellet. Cells were lysed in 350 µL RLT buffer (Qiagen, Germantown, MD, USA) and frozen at –80 ℃ for RNA extraction. Remaining SF was aliquoted in 200 µL aliquots and frozen at –80 ℃ for cytokine analyses.

Whole blood (20 mL) was obtained using a 20-gauge 1.5-inch needle and 20 mL syringe from the jugular vein following septic preparation. PBMCs were isolated from whole blood by density gradient centrifugation (Ficoll-Paque TM plus, GE Healthcare Bio-Sciences), washed in phosphate-buffered saline, and centrifuged at 2,000 rpm at 8 ℃ for 10 minutes to obtain a cell pellet. Cells were lysed in 350 µL RLT buffer (Qiagen, Germantown, MD, USA) and frozen at –80 ℃ for RNA extraction.

RNA was extracted from frozen synovial and PBMC cell pellets using the RNAeasy kit (Qiagen Germantown, MD, USA) according to manufacturer's instructions and sent to Novogene Corporation Inc. (Sacramento, CA, USA) for bulk RNA sequencing. RNA quality was determined by bioanalyzer (Agilent Technologies, Santa Clara, CA, USA). mRNA was enriched using oligo (dT) beads, followed by cDNA library generation using TruSeq RNA Library Prep Kit (Illumina, San Diego, CA, USA). Sequencing was performed on Illumina Novaseq 6000 machine using 150 bp paired end reads.

Cytokine analyses

Fluorescent bead-based multiplex assay (Milliplex MAP Equine Cytokine/Chemokine Magnetic Beads Multiplex Assay, Millipore Sigma, Burlington, MA, 01803) was used to quantify the concentrations of 23 analytes [Eotaxin/CCL11, fibroblast growth factor (FGF)-2, Fractalkine/CS3CL1, granulocyte colony-stimulating factor (G-CSF), GM-CSF, growth related protein (GRO), interferon (IFN), IL-1α, IL-1β, IL-2, IL-4, IL-5, IL-6, IL-8/CXCL8, IL-10, IL-12 (p70), IL-13, IL-17a, IL-18, IP-10, MCP-1, RANTES/CCL5 and TNFα] in SF and plasma aliquots.

Statistical analysis

To analyze microbiome data, microbial DNA was frozen at –80 ℃ and sent to ACME (Anschutz Center for Microbiome Excellence), at University of Colorado Anschutz Medical Campus, Aurora, CO for microbial sequencing. The library was prepared according to Earth Microbiome project protocol (https://earthmicrobiome.org/protocols-and-standards/16s/), using 515F and 806R primers. Samples were run on Illumina Miseq sequencing instruments. Microbial sequence analyses were performed with QIIME2 (version QUIIM2-2022.8, classifier green genes gg-13-8-99-515-806-nb-classifer) (33). Microbial community similarity was displayed with principal coordinate analysis (PCoA) plots. Alpha diversity was determined using Shannon, Faith, and pielou indices. Beta diversity using weighted and unweighted UniFrac, as well as Bray Curtis. Alpha diversity indices were compared using a paired *t*-test, and beta diversity metrics were compared with PERMANOVA. Analysis of composition of microbiomes (ANCOM) was employed to determine the sequence variants that differed significantly between treatment

groups (34). In addition, Linear discriminant analysis Effect Size (LEfSE) was also used to calculate the taxa that best discriminated between OA or healthy group (https://huttenhower.sph.harvard.edu/lefse/) (35). Microbial features were filtered for a minimum frequency of 150 were removed and features not present in >3 samples were also removed, resulting in a total of 972 total features. Median frequency for n=18 samples was 36,952.5 and total frequency was 681,082. Correlative analyses were performed to determine microbial clades associated with OA status, age, and body condition.

To analyze RNA sequencing data, demultiplexed Fasq reads generated by Novogene were analyzed using Partek® Flow® software, v10.0 (Partek Inc. Chesterfield, MO, USA). Reads were trimmed for Phred score of 20, adapters removed using cutadapt (36). Trimmed reads were aligned using STAR 2.7.3 using EquCab3.0 and annotated with Ensembl EquCab3.0.107. Feature counts were generated with HTseq (37). Differential analysis was computed using counts normalized to CPM, using DESeq (6). Pathway analysis was performed with Gene Set Enrichment Analysis (GSEA) v4.2.1 using Hallmark pathways (38).

To analyze cytokine data, age, and body condition score between horses with and without OA, raw data was plotted and visually assessed for normality prior to statistical analyses. Unpaired nonparametric Kolmogorov-Smirnov *t*-tests were used to compare cumulative distributions. Statistical analyses, graphical analyses and graph generation were performed using Prism software v8.4.1 (GraphPad Software Inc., La Jolla, CA). For all analyses, statistical significance was assessed as $P<0.10$ due to small sample size.

To perform interactome correlation of transcriptome to microbiome data, significant differentially expressed genes (DEGs) were extrapolated from the RNA sequencing data, these genes were then filtered for an average normalized expression of >100 reads, correlation analysis input included 638 genes in the SF RNAseq and 97 genes from the PBMC RNAseq. The median ratio normalized reads from individual samples were then correlated to the percent relative abundance of 45 unique bacterial genus found in n=12 samples (healthy and OA) using rcorr (39,40). P values for significance and r values for correlation were generated for each gene to genus pair. Protein coding genes with correlations P values ≤0.05 were then entered into string protein database (https://string-db.org) (41) for categorizing the protein sets. Significantly correlated genes from the PBMC DEGs did not yield any common categories, therefore we focused on the SF transcriptome to microbiome correlations.

Results

Horses

Sixty-two horses were initially enrolled based on population-based sampling that presented to the Colorado State University Veterinary Teaching Hospital. Horses (n=31) identified as having OA ranged in age from 2 to 22 (median 15 years) and included 1 Paint, 3 Arabians, 3 Warmbloods, and 24 Quarter Horses, with 13 gelding, 2 stallions, and 15 mares. Horses identified as controls were Quarter Horses ranging in age from 2 to 4 (median 3 years) and included 17 geldings and 14 mares. Horses identified as having the most severe cases of OA that underwent arthroscopy and had SF available for transcriptomic correlations to microbial abundance were further evaluated and compared to available control horses. Further correlative analyses were performed to assess the effect of age and body condition on microbial abundance relative to OA status.

Six horses (5 Quarter Horses, 1 Arabian; age 7 to 15 years, median 12 years; 2 mares, 4 geldings) were identified with severe OA that underwent arthroscopic surgical evaluation. Twelve Quarter Horses (age 2 to 3 years, median 2.75 years; 6 mares, 6 geldings) for which SF was available were identified as study controls to perform further transcriptomic analyses and correlations to microbiome data. All horses were skeletally mature based on survey radiographs of the sampled joint. In this limited group, age was significantly greater in horses with severe OA compared to healthy horses (P=0.001). Body condition score of horses with severe OA (median 6/9, range 5 to 8/25) was significantly higher (P=0.009) than that of healthy horses (median 4/9 range 3 to 5).

SF samples for comparative transcriptomic analysis to microbiomic outcomes were obtained from the tibiotarsal joint in all cases for healthy horses and from the radiocarpal in 4/6 cases, tibiotarsal in 1/6 cases and femorotibial in 1/6 cases in OA horses. SF volume obtained did not differ between groups (control cases range 3 to 10 mL, mean 7.1 mL, SD 2.7; OA cases range 4 to 7 mL, mean 5.2 mL, SD 1.3).

Transcriptomic and cytokine analyses

Comparison of transcriptomes of SF cells from OA versus healthy horses revealed marked changes, including upregulation of 810 genes and downregulation of 352 genes with fold change ≥2 or ≤–2 and significant FDR (false discovery rate) adjusted P value of ≤0.05 (*Figure 2A*,*2B*, table available at https://cdn.amegroups.cn/static/public/atm-24-109-1.xlsx). Sufficient RNA for sequencing was available

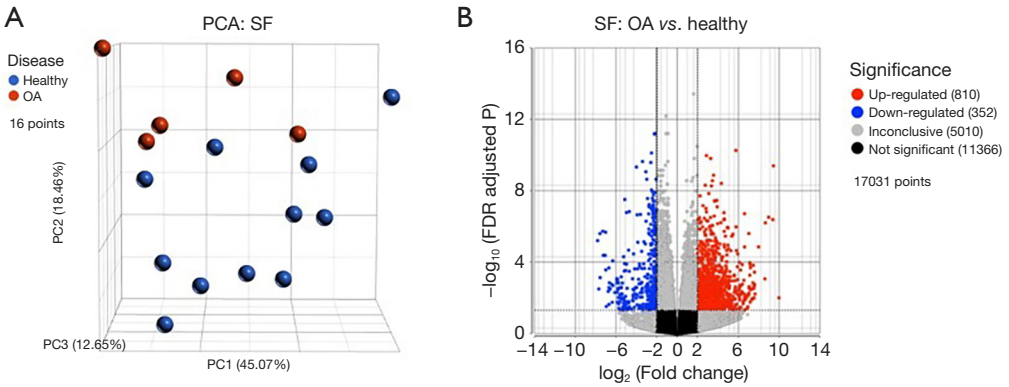

C

Gene ID	Description	FDR (OA *vs.* healthy)	Log_2 (FC) (OA *vs.* healthy)
ENSECAG00000030788	Eukaryotic Translation Initiation Factor 4E Type 3	1.01E−02	9.99
SPHKAP	A-kinase anchor protein SPHKAP	4.02E−10	9.44
DEFB4B	Beta-defensin 4A	4.17E−07	9.39
HTR2A	5-hydroxyiryptamine receptor 2A	3.08E−07	8.98
HOXD10	Homeobox protein Hox-D10	6.31E−07	8.65
ENSECAG00000008562	Uncharacterized protein	8.72E−04	8.60
RBPMS2	RNA-binding protein with multiple splicing 2	1.41E−05	7.99
ENSECAG00000034859	Zinc finger protein 596-ike	6.04E−03	7.64
FAM47E	Protein FAM47E	1.82E−03	7.60
SIX4	Homeobox protein SIX4	3.68E−04	7.59
SYN3	Synapsin-3	1.00E−02	7.54
HOXD11	Homeobox protein Hox-D11	2.24E−03	7.54
GBX2	Homeobox protein GBX-2	2.96E−03	7.52
SAMD5	Sterile alpha motif domain-containing protein 5	1.52E−04	7.47
POPDC3	Popeye domain-containing protein 3	1.46E−03	7.44
ENSECAG00000033643	Protein S100-A8	1.18E−02	7.41
MAGI2	Membrane-associated guanylate kinase, WW and PDZ domain-containing protein 2	3.33E−03	7.34
PIP4P2	Type 2 phosphatidylinositol 4, 5-bisphosphate 4-phosphatase	1 21E−02	7.31
NRXN1	Neurexin-1	2.07E−04	7.20

D

Gene ID	Description	FDR (OA *vs.* healthy)	Log_2 (FC) (OA *vs.* healthy)
ENSECAG00000043054	Ig-like domain-containing protein	6.26E−06	−7.80
ASTN2	Astrotactin-2	3.21E−03	−7.69
TNK1	Non-receptor tyrosine-protein kinase TNK1	2.53E−06	−7.57
CXCL13	C-X-C motif chemokine 13	7.40E−04	−7.57
KIAA0319	Dyslexia-associated protein KIAA0319	1.86E−06	−7.31
ANKDD1A	Ankyrin repeat and death domain-containing protein 1A	4.16E−05	−7.25
CLEC4F	C-type lectin domain family 4 member F	4.17E−05	−7.07
SYT8	Synaptotagmin-8	2.13E−06	−7.03
MZB1	Marginal zone B- and B1-cell-specific protein	2.72E−04	−7.01
ATP13A4	Probable cation-transporting ATPase 13A4	3.09E−02	−6.95
ENSECAG00000042217	IGv domain-containing protein	4.43E−03	−6.76
BHLHA15	Class A basic helix-loop-helix protein 15	2.71E−03	−6.70
MEI1	Meiosis inhibitor protein 1	2.15E−04	−6.70
IL5RA	Interieukin-5 receptor subunit alpha	2.35E−02	−6.69
ENSECAG00000043002	Ig-like domain-containing protein	3.27E−03	−6.57
ENSECAG00000022264	Ig-like domain-containing protein	1.75E−03	−6.42
ENSECAG00000037919	C-type lectin domain family 7 member A-like	1.79E−02	−6.37
ENSECAG00000037583	Ig-like domain-containing protein	8.56E−05	−6.32
TRAV29DV5	T cell receptor alpha variable 29/delta variable 5	2.08E−03	−6.31
COL20A1	Collagen alpha-1(XX) chain	5.09E−03	−6.11

Figure 2 RNA sequencing analysis comparing transcriptomes of synovial fluid cells from horses with and without OA. (A) PCA or normalized counts from synovial cells. Blue dots show n=11 biological replicates of healthy horses and red dots show n=5 biological replicates of OA horses with sufficient RNA for sequencing. (B) Volcano plot of synovial fluid from OA versus healthy horses. X-axis shows fold change and y-axis shows FDR adjusted P value, with significantly upregulated genes shown as red dots and significantly downregulated genes shows as blue dots. Significance defined as FDR ≤0.05 fold change ≥2 or ≤−2. Differential gene expression of synovial fluid cells from OA versus healthy horses. List of genes, description, unadjusted P value and fold-change of top 20 (C) upregulated and (D) downregulated genes in differential analysis results from OA versus healthy horses. PCA, principal component analysis; SF, synovial fluid; OA, osteoarthritis; FC, fold change; FDR, false discovery rate.

from n=5 OA horses and n=11 healthy horses. The most upregulated genes in synovial cells of OA horses included those related to translation initiation in protein synthesis (ENSECAG), cyclic adenosine 3'-5' monophosphate (cAMP) signaling (A-kinase anchor protein), inflammatory response and host defense at epithelial and mesenchymal surfaces (DEFB4B), serotonin receptor expression (HTR2A) and gene transcription (HOXD10, HOXD11, GBX2) (*Figure 2C*). Downregulated genes mapped to categories including structural stability (ENSECAG00000030788), neuronal migration (ASTN2, KIAA0319), intracellular signaling (TNK1), chemotaxis (CXCL13) (*Figure 2D*). Pathway analysis revealed that OA disease processes triggered significant upregulation of epithelial-mesenchymal transition pathways associated with loss of cell polarization and basement membrane interaction, oxidative phosphorylation, Myc targets involved in regulation of gene transcription involved in cell growth and proliferation, as well as adipogenesis, glycolysis and fatty acid metabolism (*Figure 3A,3B*).

In SF, cytokine concentrations were measurable for 17 cytokines evaluated (FGF-2, eotaxin, G-CSF, IL-13, IL-5, IL-18, IL-1β, IL-6, IL-17A, IL-4, IL-12, IFN-γ, IP-10, GRO, MCP-1, IL-10, TNF-α). Significant differences were seen between horses with and without OA with elevated cytokine levels in horses with OA for 6 cytokines: IL-1β (P=0.02), IL-6 (P=0.005), G-CSF (P=0.02), IP-10 (P=0.08), IL-17A (P=0.09), and IL-18 (P=0.09) (*Figure 3C*).

Comparison of transcriptomes of PBMC isolated from OA versus healthy horses revealed moderate changes, including upregulation of 41 genes and downregulation of 55 genes with fold change ≥2 or ≤–2 and significant FDR (false discovery rate) adjusted P value of ≤0.05 (*Figure 4A,4B*, table available at https://cdn.amegroups.cn/static/public/atm-24-109-2.xlsx). Sufficient RNA for sequencing was available from n=6 OA horses and n=8 healthy horses. The most upregulated genes in PBMC of OA horses included those related to cell cycle progression and neuronal differentiation (DMRTA2), reverse transcriptase (ENSECAG00000037442) and acute phase response (ENSECAG00000021580) (*Figure 4C*). Downregulated genes mapped to categories including collagen dysregulation (COL28A1), epidermal and lymph development (SVEP1) and NAD synthesis implicated in neurodegenerative disorders (ACMSD) (*Figure 4D*). Pathway analysis revealed that OA disease processes triggered significant upregulation of inflammatory responses, eicosanoid and complement pathways associated with inflammation, immune response and cell proliferation, protein secretion, TNF-α, IL-2 and IL-6 Jak Stat3 signaling and downregulation of mTORC1 signaling (*Figure 5A,5B*). Upregulation of IL-6 and IL-2 pathways were reflected in elevated cytokine levels detected via multiplex immunoassay as well.

In plasma, cytokine concentrations were measurable for 19 cytokines (FGF-2, eotaxin, G-CSF, IL-1α, fractalkine, IL-5, IL-18, IL-1β, IL-6, IL-17A, IL-2, IL-4, IL-12, IFN-γ, IL-8, IP-10, GRO, IL-10, TNF-α). Significant differences were seen between horses with and without OA with elevated cytokine levels in horses with OA for 6 cytokines: IFN-γ (P=0.004), IL-18 (P<0.001), IL-6 (P=0.02), IP-10 (P=0.02), IL-2 (P=0.09), and G-CSF (P=0.09) (*Figure 5C*).

Further comparison of gene expression pathways that were up- or downregulated in both SF cells and PBMCs was performed (*Figure 6A-6C*). Findings yielded 111 pathways that were upregulated in both SF cells and PBMC, and 34 pathways that were downregulated in both cell lines. Several of the most upregulated pathways mapped to processes related to cell communication, cellular response to stimuli and movement of cells or subcellular components. Several of the most downregulated pathways mapped to metabolic, cellular, and immune system related processes, response to stimuli and biological regulation (*Figure 6D-6G*).

Fecal microbiome comparison between OA and healthy horses

The predominant bacterial phyla present in equine feces of horses both with and without OA were *Firmicutes* and *Bacteroidetes* (*Figure 7A-7C*). PCoA using Bray-Curtis dissimilarity for beta diversity quantification of differences allowed visualization of overall bacterial taxonomic composition from fecal samples from horses with and without OA, demonstrating distinct grouping of OA samples (red) compared to healthy controls (blue) (*Figure 7D*). PERMANOVA testing identified significant differences in beta-diversity comparing horses with OA to controls (P=0.003). Faith alpha diversity was also significantly reduced (P=0.02) in horses with OA compared to healthy controls (*Figure 7E*). ANCOM Differential analysis of microbial populations between OA and Healthy control feces revealed a statistically significant higher abundance of class *Epsilonproteobacteria*, order *Campylobacteria* and also family *Dehalobacteriaceae* in the OA feces, whereas there was a statistically significant lower abundance of phylum *Lentisphaerae* and also genus *Sarcina* in the healthy feces

A

SF pathway OA *vs.* HC	Size	Normalized enrichment score	P-val	FDR q-val
HALLMARK_EPITHELIAL_MESENCHYMAL_TRANSITION	182	3.2192771	0	0
KEGG_RIBOSOME	72	3.1008787	0	0
HALLMARK_OXIDATIVE_PHOSPHORYLATION	183	3.0689971	0	0
KEGG_OXIDATIVE_PHOSPHORYLATION	102	2.8002844	0	0
HALLMARK_MYC_TARGETS_V1	180	2.776735	0	0
KEGG_PARKINSONS_DISEASE	100	2.7276144	0	0
KEGG_HUNTINGTONS_DISEASE	154	2.7037926	0	0
HALLMARK_ADIPOGENESIS	185	2.6050258	0	0
HALLMARK_GLYCOLYSIS	181	2.5926785	0	0
HALLMARK_FATTY_ACID_METABOLISM	138	2.477124	0	0
HALLMARK_HYPOXIA	186	2.4737847	0	0
KEGG_PENTOSE_PHOSPHATE_PATHWAY	21	2.2558498	0	0
KEGG_CITRATE_CYCLE_TCA_CYCLE	29	2.2498655	0	0
HALLMARK_ANGIOGENESIS	30	2.242871	0	0
KEGG_ALZHEIMERS_DISEASE	143	2.2418294	0	0
KEGG_GLYCOLYSIS_GLUCONEOGENESIS	47	2.2403088	0	0
HALLMARK_MTORC1_SIGNALING	190	2.1901846	0	0
KEGG_AMINO_SUGAR_AND_NUCLEOTIDE_SUGAR_METABOLISM	41	2.1567936	0	1.27E−04
HALLMARK_COAGULATION	109	2.1516032	0	0
KEGG_DRUG_METABOLISM_CYTOCHROME_P450	25	2.1090484	0	4.63E−04

B

SF pathway OA *vs.* HC	Size	Normalized enrichment score	P-val	FDR q-val
HALLMARK_INTERFERON_ALPHA_RESPONSE	89	−3.0549412	0	0
HALLMARK_INTERFERON_GAMMA_RESPONSE	177	−2.8585305	0	0
HALLMARK_ALLOGRAFT_REJECTION	177	−2.4279068	0	0
BIOCARTA_NO2IL12_PATHWAY	15	−2.3909066	0	0
BIOCARTA_CTLA4_PATHWAY	17	−2.237048	0	5.21E−04
BIOCARTA_CSK_PATHWAY	16	−2.1814635	0	7.91E−04
BIOCARTA_TOB1_PATHWAY	19	−2.1061726	0	0.00343341
BIOCARTA_TCR_PATHWAY	42	−2.0850925	0	0.00382471
BIOCARTA_IL2RB_PATHWAY	36	−2.0724895	0.002070393	0.00340565
BIOCARTA_IL12_PATHWAY	19	−2.0532255	0	0.00360023
BIOCARTA_IL7_PATHWAY	16	−2.0455074	0	0.0031502
BIOCARTA_TNFR2_PATHWAY	17	−2.0252967	0	0.00393512
BIOCARTA_CD40_PATHWAY	15	−2.019683	0.00204499	0.00391816
BIOCARTA_41BB_PATHWAY	18	−1.9585747	0.002028398	0.00687636
BIOCARTA_KERATINOCYTE_PATHWAY	45	−1.9335026	0.001988072	0.00877299
BIOCARTA_STATHMIN_PATHWAY	18	−1.8982273	0.002173913	0.01186104
BIOCARTA_MCM_PATHWAY	18	−1.8754721	0.00204918	0.01409677
BIOCARTA_STRESS_PATHWAY	24	−1.8342705	0	0.02010616
BIOCARTADEATH_PATHWAY	28	−1.8071697	0.002132196	0.02403028
BIOCARTA_ATRBRCA_PATHWAY	21	−1.7714088	0.002028398	0.03004018

C

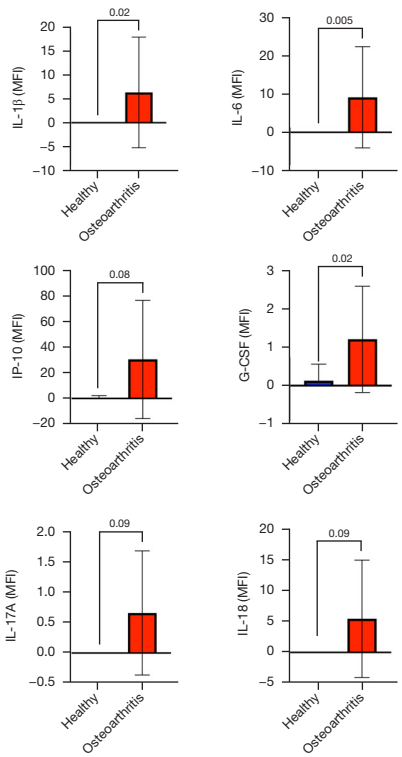

Figure 3 Pathway analysis of differential gene expression of synovial cells and synovial fluid cytokine expression profiles from horses with and without OA. Pathway analyses were determined using normalized counts from n=11 biological replicates of healthy horses and n=5 OA horses indicating the top 20 (A) upregulated and (B) downregulated pathways. With unadjusted P value and FDR adjusted P value (q-value) shown in table. (C) Cytokine levels in synovial fluid were determined via multiplex immunoassay. Y-axis shows MFI of each cytokine. In synovial fluid, cytokine concentrations were measurable for 17 cytokines (FGF-2, eotaxin, G-CSF, IL-13, IL-5, IL-18, IL-1β, IL-6, IL-17A, IL-4, IL-12, IFN-γ, IP-10, GRO, MCP-1, IL-10, TNF-α). Significant differences were seen between horses with and without OA with elevated cytokine levels in horses with OA for 6 cytokines (IL-1β, IL-6, IP-10, G-CSF, IL-17A, IL-18). Bars are mean and standard deviation of biological replicates performed in duplicate. Due to small sample size, significance was assessed at P<0.1. SF, synovial fluid; OA, osteoarthritis; HC, healthy control; FDR, false discovery rate; MFI, mean fluorescence intensity; KEGG, Kyoto Encyclopedia of Genes and Genomes; FGF, fibroblast growth factor; G-CSF, granulocyte colony-stimulating factor; IL, interleukin; IFN-γ, interferon gamma; IP-10, interferon gamma inducible protein 10; GRO, growth related protein; MCP-1, monocyte chemoattractant protein-1; TNF-α, tumor necrosis factor-α.

(*Figure 8A-8E*).

LEfSe also identified an additional 11 genera that are significantly higher in abundance in the OA samples (*Akkermansia*, *Campylobacter*, *p75a5*, *Phascolarctobacterium*, *Oscillospira*, *Pseudobutyrivibrio*, *Dorea*, *Butyrivibrio*, *Blautia*, *Ruminococcus*, *Mogibacterium*) and 6 additional genera that are significantly higher in abundance in the healthy feces (*Anaeroplasma*, *RFNN20*, *Epulopiscium*, *Sarcina*, *Clostridium*, *Fibrobacter*, *BF311*) (*Figure 8F*). Due to the higher median BCS and age of the OA horses compared to the 12 healthy controls, a larger cohort of OA horses (n=29) with 16S data available was used to perform correlations between genus level relative abundance, BCS and age. Of the above genera, 3 of the OA enriched (*Blautia*, *Phascolarctobacterium*, *Dorea*) and 4 of the heathy enriched genera (*Clostridium*, *Sarcina*, *Fibrobacter*, *Anaeroplasma)* were not correlated with age or body condition, indicating the differential abundance appeared solely attributed to OA status (*Table 1*). When this larger OA population (n=29) was examined for relative abundance of microbial taxa by age (< or ≥15 years) or body condition (< or ≥5 on 9-point scale), there was no difference in relative abundance of microbial taxa by ANCOM or

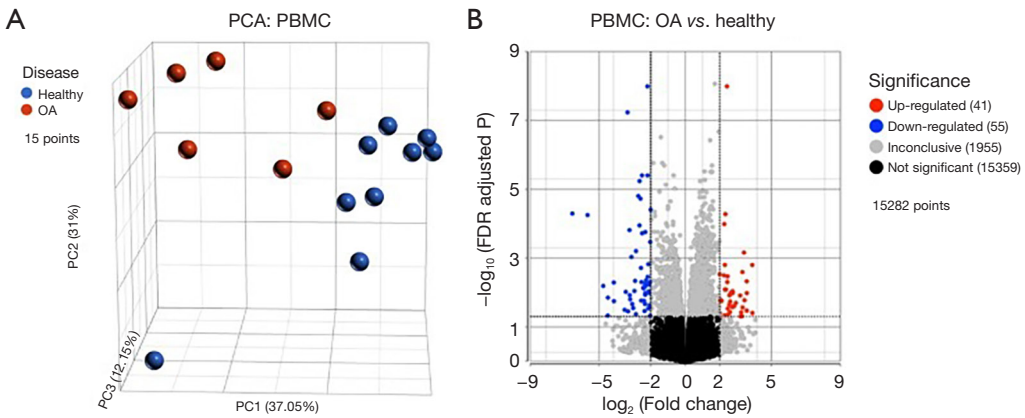

C

Gene ID	Description	FDR (OA *vs.* healthy)	Log_2 (FC) (OA *vs.* healthy)
DMRTA2	Doublesex- and mab-3-related transcription factor A2	3.96E−02	3.90
ENSECAG00000037442	Reverse transcriptase domain-containing protein	1.60E−03	3.89
ENSECAG00000021580	Haptoglobin	1.05E−02	3.57
GYS2	Glycogen [starch] synthase, liver	3.40E−02	3.57
NOVA1	RNA-binding protein Nova-1	4.75E−03	3.57
LIFR	Leukemia inhibitory factor receptor	1.69E−02	3.44
ABCC13	ATP Binding Cassette Subfamily C Member 13 (Pseudogene)	6.97E−04	3.41
SDR9C7	Short-chain dehydrogenase/reductase family 9C member 7	2.76E−02	3.33
RTN1	Reticulon-1	2.56E−03	3.32
OLR1	Oxidized low-density lipoprotein receptor1	4.94E−02	3.29
FOXO6	Forkhead box protein O6	3.83E−02	3.25
MFAP3L	Microfibrillar-associated protein 3-like	1.23E−02	3.19
SLC4A1	Band 3 anion transport protein	2.03E−02	2.94
FN1	Fibronectin	2.49E−02	2.84
SPRY3	Protein sprouty homolog 3	1.04E−02	2.75
ENSECAG00000021060	Family with sequence similarity 209 member B	2.676−02	2.73
ENSECAG00000038377	Reverse transcriptase domain-containing protein	1.06E−02	2.64
ALAS2	5-aminolevulinate synthase, erythroid-specific, mitochondrial	1.85E−02	2.61
WNT11	Protein wnt-11	3.75E−02	2.60
OLFM4	Clfactomedin-4	1.22E−02	2.57

D

Gene ID	Description	FDR (OA *vs.* healthy)	Log_2 (FC) (OA *vs.* healthy)
COL28A1	Collagen alpha-1 (XXVIIII) chain	5.11E−05	−6.55
SVEP1	Sushi, von Willebrand factor type A, EGF and pentraxin domain-containing protein 1	5.65E−05	−5.67
ACMSD	2-amino-3-carboxymuconate-6-semialdehyde decarboxylase	6.49E−03	−4.76
ARPP21	cAMP-regulated phosphoprotein 21	4.71E−02	−4.50
H2BC7	H2B Clustered Histone 7	1.42E−02	−4.49
GAL	Galanin peptides	5.16E−03	−4.15
ADAMTSL2	ADAMTS like 2	1.80E−02	−4.14
RIMKLA	N-acetylaspartylglutamate synthase A	3.21E−02	−3.52
ENSECAG00000040754	Ig-like domain-containing protein	9.67E−03	−3.45
ENSECAG00000019204	Fc receptor-like protein 5	5.86E−08	−3.35
SYT17	Synaplobagmin-17	3.56E−02	−3.32
STMN2	Stathmin-2	1.55E−04	−3.24
RPRML	Reprimo-like protein	1.21E−02	−3.22
ANGPT4	Angiopoietin-4	1.59E−02	−3.20
PRDMM16	Histone-lysine N-methyltransferase PRDM16	9.39E−04	−3.12
ESRRB	Steroid hormone receptor ERR2	2.19E−02	−3.07
NEU4	Sialidase-4	2.85E−02	−3.02
ENSECAG00000015137	Granzyme B-like	9.11E−03	−2.95
KCNF1	Potassium voltage-gated channel subfamily F member 1	4.63E−03	−2.91
TBX1	T-box transcription factor TBX1	4.28E−02	−2.86

Figure 4 RNA sequencing analysis comparing transcriptomes of PBMCs from horses with and without OA. (A) PCA or normalized counts from synovial cells. Blue dots show n=9 biological replicates of healthy horses and red dots show n=6 biological replicates of OA horses with sufficient RNA for sequencing. (B) Volcano plot of PBMC from OA versus healthy horses. X-axis shows fold change and y-axis shows FDR adjusted P value, with significantly upregulated genes shown as red dots and significantly downregulated genes shows as blue dots. Significance defined as FDR ≤0.05 fold change ≥2 or ≤−2. Differential gene expression of peripheral blood mononuclear cells from OA versus healthy horses. List of genes, description, unadjusted P value and fold-change of top 20 (C) upregulated and (D) downregulated genes in differential analysis results from OA versus healthy horses. PCA, principal component analysis; PBMC, peripheral blood mononuclear cell; OA, osteoarthritis; FDR, false discovery rate; FC, fold change.

A

PBMC OA *vs.* HC	Size	Normalized enrichment score	P-val	FDR q-val
KEGG_LYSOSOME	115	2.5544832	0	0
KEGG_GLYCOSAMINOGLYCAN_DEGRADATION	17	2.2733457	0	0
KEGG_ABC_TRANSPORTERS	35	2.069888	0	0.002262053
BIOCARTA_MET_PATHWAY	33	2.0170708	0	0.026012095
HALLMARK_INFLAMMATORY_RESPONSE	180	2.0025976	0	0
BIOCARTA_EICOSANOID_PATHWAY	22	1.9942101	0	0.016933085
KEGG_STARCH_AND_SUCROSE_METABOLISM	28	1.9791983	0	0.005159383
HALLMARK_COMPLEMENT	166	1.970756	0	0
KEGG_DORSO_VENTRAL_AXIS_FORMATION	21	1.9584537	0.001779359	0.005917874
HALLMARK_PROTEIN_SECRETION	89	1.9366769	0	7.61E−04
HALLMARK_TNFA_SIGNALING_VIA_NFKB	187	1.9330205	0	5.70E−04
KEGG_TYPE_II_DIABETES_MELLITUS	44	1.9236348	0	0.007047779
HALLMARK_KRAS_SIGNALING_UP	181	1.9191476	0	6.81E−04
BIOCARTA_ARAP_PATHWAY	17	1.9026546	0	0.0328821
KEGG_GNRH_SIGNALING_PATHWAY	90	1.882197	0	0.010054772
KEGG_INSULIN_SIGNALING_PATHWAY	123	1.8552998	0	0.013421381
HALLMARK_COAGULATION	108	1.8432258	0	0.001694513
KEGGRENAL_CELL_CARCINOMA	67	1.8351818	0	0.016849132
HALLMARK_HEDGEHOG_SIGNALING	33	1.8336363	0.001692047	0.00145244
KEGG_SPHINGOLIPID_METABOLISM	36	1.8182162	0.003267974	0.017918825

B

PBMC OA *vs.* HC	Size	Normalized enrichment score	P-val	FDR q-val
HALLMARK_E2F_TARGETS	188	−3.7676501	0	0
KEGG_RIBOSOME	71	−3.3349211	0	0
HALLMARK_MYC_TARGETS_V1	180	−3.276198	0	0
HALLMARK_G2M_CHECKPOINT	184	−3.2603867	0	0
KEGG_DNA_REPLICATION	34	−3.1270099	0	0
BIOCARTA_MCM_PATHWAY	17	−2.7622025	0	0
KEGG_SPLICEOSOME	117	−2.7196891	0	0
HALLMARK_DNA_REPAIR	137	−2.692242	0	0
KEGG_MISMATCH_REPAIR	22	−2.650606	0	0
KEGG_HOMOLOGOUS_RECOMBINATION	27	−2.4732869	0	0
KEGG_NUCLEOTIDE_EXCISION_REPAIR	40	−2.4636338	0	0
KEGG_PROTEASOME	40	−2.377775	0	1.11E−04
HALLMARK_MYC_TARGETS_V2	56	−2.3544772	0	0
KEGG_BASEEXCISION_REPAIR	32	−2.3456354	0	9.75E−05
KEGG_CELL_CYCLE	118	−2.2978208	0	8.66E−05
KEGG_PRIMARY_IMMUNODEFICIENCY	33	−2.2974653	0	7.80E−05
KEGG_PARKINSONS_DISEASE	101	−2.2874262	0	7.09E−05
KEGG_RNA_POLYMERASE	23	−2.1654286	0	2.47E−04
KEGG_PYRIMIDINE_METABOLISM	84	−2.1421366	0	2.90E−04
BIOCARTA_PROTEASOME_PATHWAY	18	−1.9287531	0	0.021158677

C

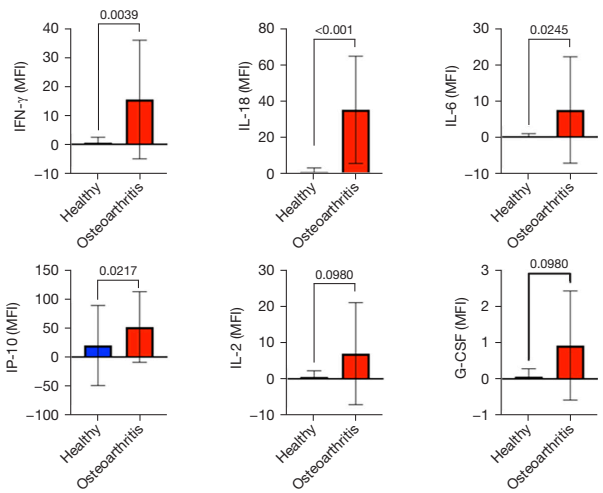

Figure 5 Pathway analysis of differential gene expression of peripheral blood mononuclear cells and cytokine expression profiles in plasma from horses with and without OA. Pathway analyses were performed using normalized counts from n=9 biological replicates of HC horses and n=6 OA horses indicating the top 20 (A) upregulated and (B) downregulated pathways. With unadjusted P value and FDR adjusted P value (q-value) shown in table. (C) Cytokine levels in plasma were determined via multiplex immunoassay. Y-axis shows MFI of each cytokine. Cytokine concentrations were measurable for 19 cytokines (FGF-2, eotaxin, G-CSF, IL-1α, fractalkine, IL-5, IL-18, IL-1β, IL-6, IL-17A, IL-2, IL-4, IL-12, IFN-γ, IL-8, IP-10, GRO, IL-10, TNF-α). Significant differences were seen between horses with and without OA with elevated cytokine levels in horses with OA for 6 cytokines: IFN-γ, IL-18, IL-6, IP-10, IL-2, and G-CSF. Bars are mean and standard deviation of biological replicates performed in duplicate. Due to small sample size, significance was assessed at P<0.1. PBMC, peripheral blood mononuclear cell; HC, healthy control; FDR, false discovery rate; KEGG, Kyoto Encyclopedia of Genes and Genomes; MFI, mean fluorescence intensity; FGF, fibroblast growth factor; G-CSF, granulocyte colony-stimulating factor; OA, osteoarthritis; IL, interleukin; IFN-γ, interferon gamma; IP-10, interferon gamma induced protein 10; GRO, growth related protein; TNF-α, tumor necrosis factor-α.

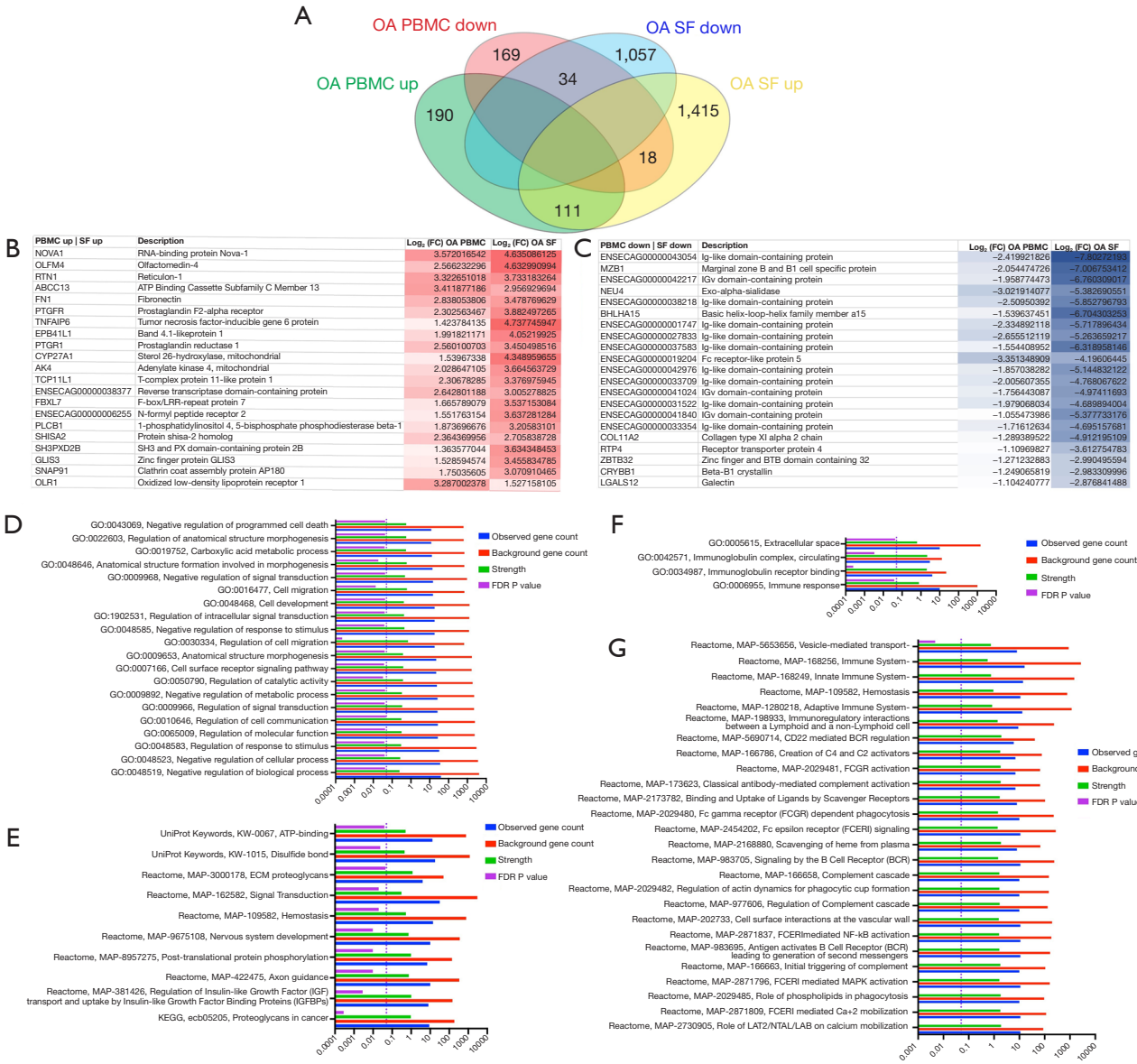

PBMC up | SF up	Description	Log_2 (FC) OA PBMC	Log_2 (FC) OA SF
NOVA1	RNA-binding protein Nova-1	3.572016542	4.635086125
OLFM4	Olfactomedin-4	2.566232296	4.632990994
RTN1	Reticulon-1	3.322851018	3.733183264
ABCC13	ATP Binding Cassette Subfamily C Member 13	3.411877186	2.956929694
FN1	Fibronectin	2.838053806	3.478769629
PTGFR	Prostaglandin F2-alpha receptor	2.302563467	3.882497265
TNFAIP6	Tumor necrosis factor-inducible gene 6 protein	1.423784135	4.737745947
EPB41L1	Band 4.1-likeprotein 1	1.991821171	4.05219925
PTGR1	Prostaglandin reductase 1	2.560100703	3.450498516
CYP27A1	Sterol 26-hydroxylase, mitochondrial	1.53967338	4.348959655
AK4	Adenylate kinase 4, mitochondrial	2.028647105	3.664563729
TCP11L1	T-complex protein 11-like protein 1	2.30678285	3.376975945
ENSECAG00000038377	Reverse transcriptase domain-containing protein	2.642801188	3.005278825
FBXL7	F-box/LRR-repeat protein 7	1.665789079	3.537153084
ENSECAG00000006255	N-formyl peptide receptor 2	1.551763154	3.637281284
PLCB1	1-phosphatidylinositol 4, 5-bisphosphate phosphodiesterase beta-1	1.873696676	3.20583101
SHISA2	Protein shisa-2 homolog	2.364369956	2.705838728
SH3PXD2B	SH3 and PX domain-containing protein 2B	1.363577044	3.634348453
GLIS3	Zinc finger protein GLIS3	1.528594574	3.455834785
SNAP91	Clathrin coat assembly protein AP180	1.75035605	3.070910465
OLR1	Oxidized low-density lipoprotein receptor 1	3.287002378	1.527158105

PBMC down | SF down	Description	Log_2 (FC) OA PBMC	Log_2 (FC) OA SF
ENSECAG00000043054	Ig-like domain-containing protein	−2.419921826	−7.80272193
MZB1	Marginal zone B and B1 cell specific protein	−2.054474726	−7.006753412
ENSECAG00000042217	IGv domain-containing protein	−1.958774473	−6.760309017
NEU4	Exo-alpha-sialidase	−3.021914077	−5.382690551
ENSECAG00000038218	Ig-like domain-containing protein	−2.50950392	−5.852796793
BHLHA15	Basic helix-loop-helix family member a15	−1.539637451	−6.704303253
ENSECAG00000001747	Ig-like domain-containing protein	−2.334892118	−5.717896434
ENSECAG00000027833	Ig-like domain-containing protein	−2.655512119	−5.263659217
ENSECAG00000037583	Ig-like domain-containing protein	−1.554408952	−6.318958146
ENSECAG00000019204	Fc receptor-like protein 5	−3.351348909	−4.19606445
ENSECAG00000042976	Ig-like domain-containing protein	−1.857038282	−5.144832122
ENSECAG00000033709	Ig-like domain-containing protein	−2.005607355	−4.768067622
ENSECAG00000041024	IGv domain-containing protein	−1.756443087	−4.97411693
ENSECAG00000031522	Ig-like domain-containing protein	−1.979068034	−4.689894004
ENSECAG00000041840	IGv domain-containing protein	−1.055473986	−5.377733176
ENSECAG00000033354	Ig-like domain-containing protein	−1.71612634	−4.695157681
COL11A2	Collagen type XI alpha 2 chain	−1.289389522	−4.912195109
RTP4	Receptor transporter protein 4	−1.10969827	−3.612754783
ZBTB32	Zinc finger and BTB domain containing 32	−1.271232883	−2.990495594
CRYBB1	Beta-B1 crystallin	−1.249065819	−2.983309996
LGALS12	Galectin	−1.104240777	−2.876841488

Figure 6 Comparison of gene expression pathways up- and downregulated in both synovial fluid cells and peripheral blood mononuclear cells of horses with OA. (A) Venn diagram of differentially expressed genes for each comparison group. (B) Top 20 shared genes upregulated in both SF and PBMC of horses with OA with fold changes listed. (C) Top 20 shared most downregulated genes in SF and PBMC with fold changes listed. (D) GO pathways represented in the 111 shared upregulated genes. Bar graphs show top 20 with observed gene count from list in blue, red bar for total genes in GO category, green bar for strength (enrichment) and purple for FDR P value (dotted line at 0.05). (E) Significant Reactome, KEGG and protein sets found in 111 upregulated gene list. (F) Significant GO pathways for 34 shared upregulated genes. (G) Significant Reactome pathways found for 34 shared downregulated genes. OA, osteoarthritis; PBMC, peripheral blood mononuclear cell; SF, synovial fluid; FC, fold change; FDR, false discovery rate; GO, Gene Ontology; KEGG, Kyoto Encyclopedia of Genes and Genomes.

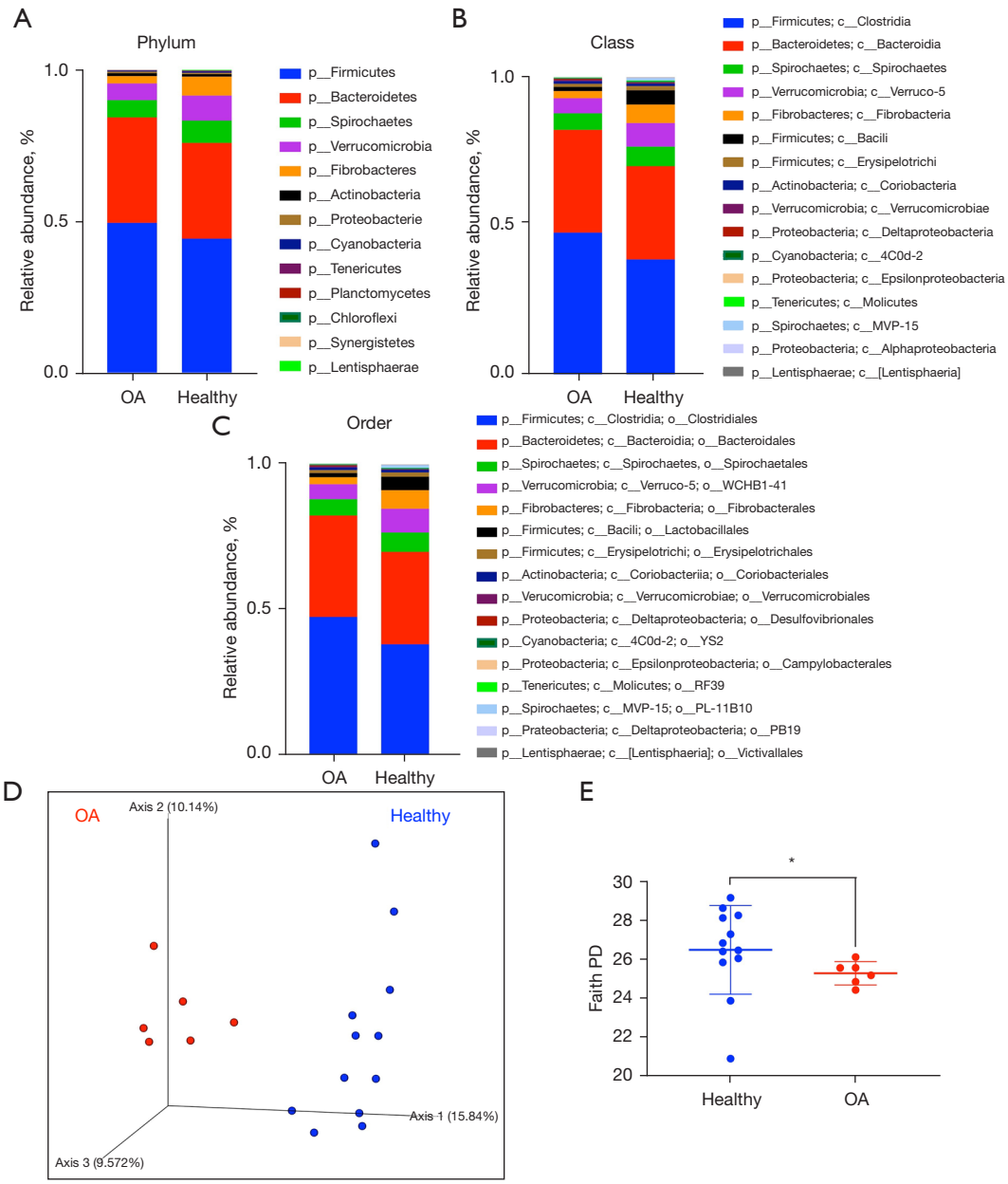

Figure 7 Fecal microbiome sequencing results. Relative abundance averaged of n=6 OA and n=12 healthy horse fecal microbial taxa. (A) Stacked bar graph of average relative abundance on phylum level with high to low shown in color scale on right. OA in left column, heathy in right column. (B) Average relative abundance on the class level. (C) Average relative abundance on the order level. (D) Bray-Curtis beta diversity plot, OA samples in red, heathy in blue. P value 0.001 by PERMANOVA. (E) Faith alpha diversity phylogenic distance measurement, P=0.04 by Kruskal-Wallis pairwise *t*-test (*, P<0.05). OA, osteoarthritis; PD, phylogenetic diversity.

alpha diversity by age or body condition. Beta diversity was demonstrated to differ by age within the OA group (P=0.007) but not body condition (P=0.20). In summary, these findings reveal that specific microbial genera are enriched in relation to OA diagnosis unrelated to differences in age or body condition between groups analyzed.

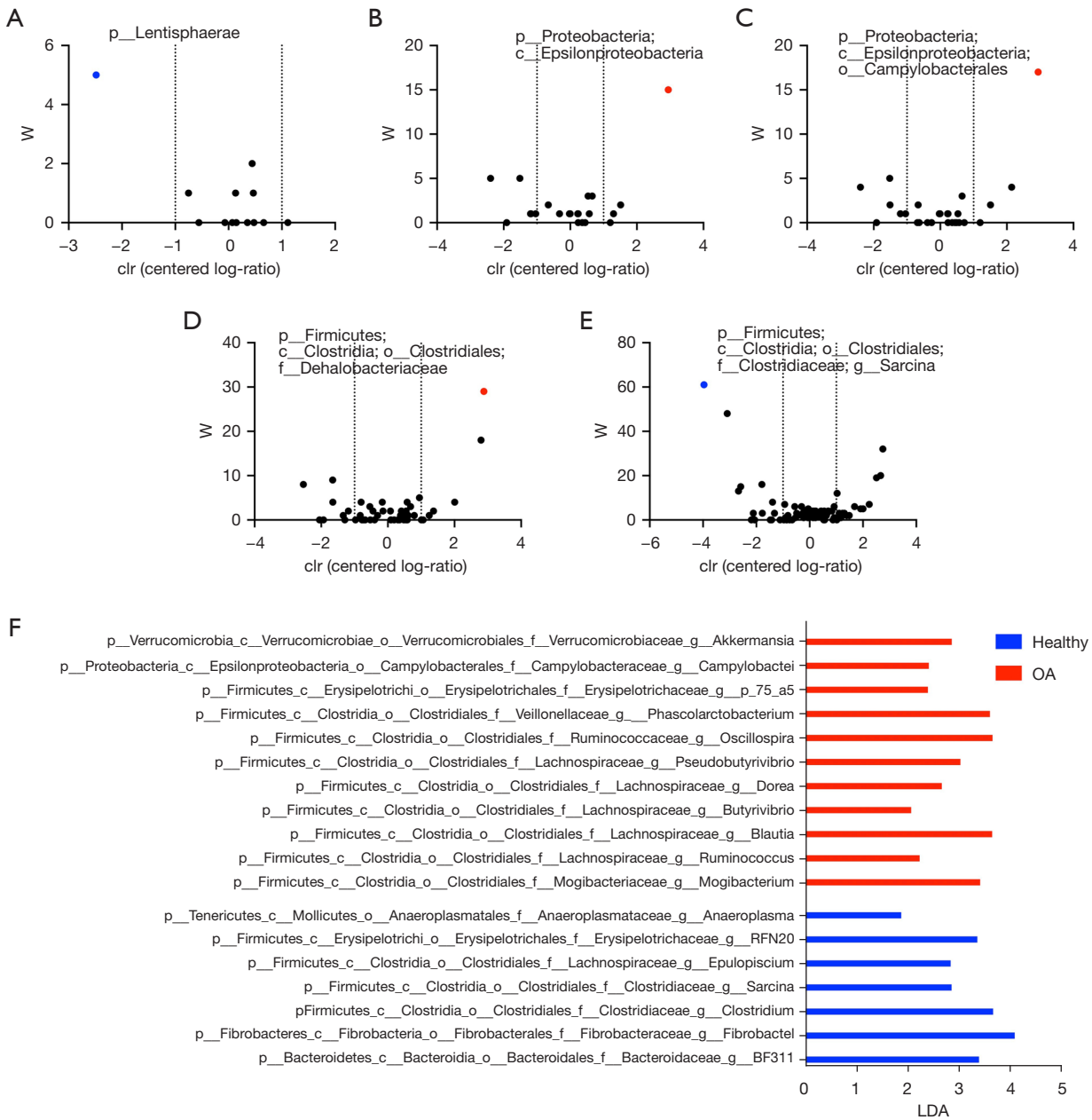

Figure 8 Differential abundance of microbial taxa in OA compared to healthy. (A) ANCOM differential analysis test of A0 phylum level taxa, blue indicated significantly lower abundance of *Lentisphaerae* in OA samples. (B) Significantly higher abundance (red) of class *Epsilonproteobacteria*. (C) Significantly higher abundance (red) of order Campylobacteria in OA samples. (D) Significantly higher abundance (red) of family *Dehalobacteriaceae* in OA. (E) Significantly lower abundance of genus *Sarcina* in OA samples. In (A-E), the W statistic represents the number of pairwise comparisons where there is a significant difference between comparisons. (F) LEfSe differential analysis results, y axis shows LDA effect size of genus level taxon, red bars show higher abundance in OA, blue bars higher abundance in healthy. OA, osteoarthritis; ANCOM, Analysis of Composition of Microbiomes; LEfSe, Linear discriminant analysis Effect Size; LDA, Linear discriminant analysis.

Table 1 Correlation analyses of microbial clades associated with osteoarthritis

Genes	Age		BCS	
	Correlation significance	Correlation r value	Correlation significance	Correlation r value
Osteoarthritis enriched				
p__Firmicutes.g__Blautia	ns	0.454	ns	0.3294
p__Firmicutes.g__Butyrivibrio	**	0.6265	ns	0.3526
p__Firmicutes.g__Epulopiscium	***	–0.7566	*	–0.5778
p__Firmicutes.g__Mogibacterium	***	0.7265	ns	0.4111
p__Firmicutes.g__Oscillospira	***	0.7299	**	0.6127
p__Firmicutes.g__p.75.a5	*	0.5389	*	0.5457
p__Firmicutes.g__Phascolarctobacterium	ns	0.4273	ns	0.3119
p__Firmicutes.g__Pseudobutyrivibrio	*	0.5415	*	0.5107
p__Firmicutes.g__Ruminococcus.	**	0.6579	ns	0.2006
p__Proteobacteria.g__Campylobacter	*	0.5737	ns	0.2795
p__Verrucomicrobia.g__Akkermansia	*	0.5682	ns	0.4587
p__Firmicutes.g__Dorea	ns	0.3298	ns	0.1017
Healthy control enriched				
p__Fibrobacteres.g__Fibrobacter	ns	–0.4195	ns	–0.456
p__Firmicutes.g__Clostridium	ns	–0.3828	ns	–0.3028
p__Firmicutes.g__RFN20	**	–0.5917	*	–0.5544
p__Firmicutes.g__Sarcina	ns	–0.4429	ns	–0.2119
p__Tenericutes.g__Anaeroplasma	ns	–0.4624	ns	–0.4257
p__Firmicutes.g__Epulopiscium	***	–0.7566	*	–0.5778
p__Bacteroidetes.g__BF311	ns	–0.3644	ns	–0.1941

Correlation analyses were performed using a larger cohort of n=29 OA horses on the differentially expressed genus shown in *Figure 8* using relative abundance correlated to BCS or age. All genera identified as correlated to OA status (*Figure 8*) are presented below; highlighting those that were not also correlated to age or body condition (i.e., highlighted genera were solely associated with OA status in this analysis) with non-significant (ns) P value or *P<0.05, **P<0.01, ***P<0.001. Pearson r values shown in table for BCS and age. Correlation analysis was performed with Graphpad Prism v10. Highlighted genera are not significantly correlated with BCS or age. OA, osteoarthritis; BCS, body condition score.

Interactome between microbial taxonomic dysregulation and differential gene expression in SF cells and PBMC in OA

To correlate the host transcriptomic responses to microbiome 639 DEGs (FC (fold change) $\geq 2\log_2$ or $\leq 2\log_2$, FDR P value ≤ 0.05) were extrapolated and paired with microbial abundance at the genus level from the same samples. Significant gene correlations were filtered for a P value ≤ 0.05, and the genus that were statistically different between OA and Healthy were selected for further analysis. In *Figure 9A* for example, the genus *Akkermansia* (phylum *Verrucomicrobia*) shows a significant correlation with 149 genes, and the genus Clostridium (lower abundance in OA) has a significant correlation with 16 genes. The r values for significantly correlated genes are shown in *Figure 9B*,*9C* for the genus that have higher abundance in OA and health, respectively, ranging from –0.6 to +0.6. To more clearly illustrate these correlation findings, the significantly correlated genes were categorized by pathway, protein type, biological and molecular processes using the

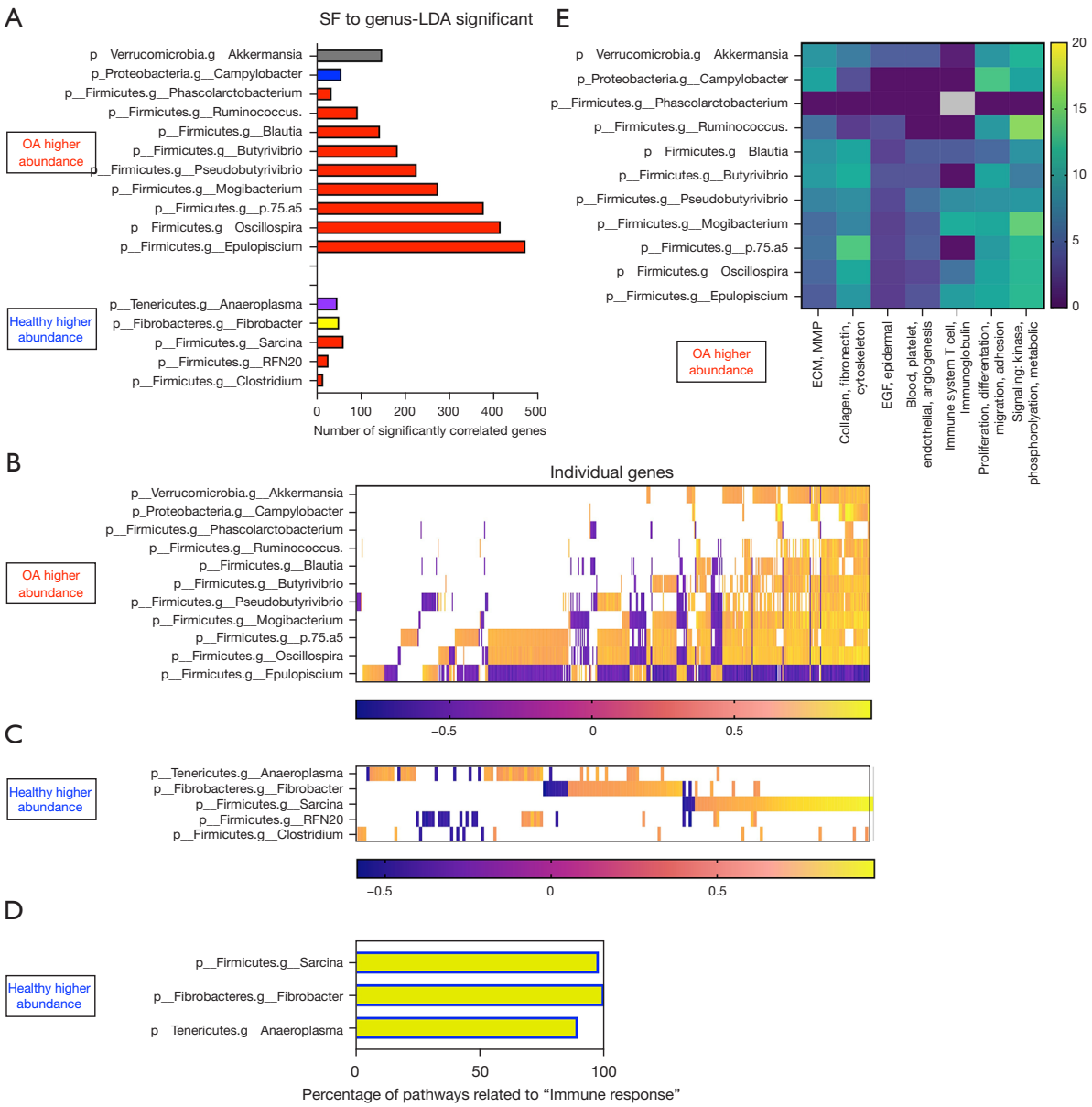

Figure 9 Immunome of OA: correlation between synovial fluid transcriptome and fecal microbiome. (A) Number of significantly correlated genes with each genus that was found to have a significantly different abundance between OA and healthy groups. Bars colored by phylum. *Firmicutes* (red), *Proteobacteria* (blue), *Verrucomicrobia* (gray), *Tenericutes* (purple) and *Fibrobacteres* (yellow). (B) For each genus significantly higher abundance in OA (11 total), the r value for correlation in shown in color scale, total of 543 genes represented on heatmap. Negative correlations in dark purple. Genes with P value <0.05 (non-significant) left blank (white). (C) For each genus with significantly higher abundance in heathy controls, the r value for correlation in shown in color scale. A total of 167 genes are represented. Color scale dark purple for negative correlation (r=−0.55), bright yellow for highest positive correlation (r=0.95). (D) Each set of genes with correlation to heathy abundant genus was categorized into STRING pathways, 3 genus shown with >90% mapped to immune related categories (specific percentage shown in bar graph). (E) For each genus significantly more abundant in OA, correlated genes were mapped to STRING categories and pathways. Heat map shows percentage of pathways with keywords shown on x axis. Grayed color for only 3 immune pathways total correlated to genus *Phascolarctobacterium*. Highest percentage in bright yellow for Ruminococcus for “signaling” category. SF, synovial fluid; LDA, Linear discriminant analysis; OA, osteoarthritis; ECM, extracellular matrix; MMP, matrix metalloproteinase; EGF, epidermal growth factor.

STRING database. Interestingly, 3 of the genera (*Sarcina*, *Fibrobacter*, *Anaeroplasma*) that have lower abundance in OA are associated exclusively with pathways related to "immune response" (*Figure 9D*), whereas the genus with a higher abundance in OA are correlated to diverse categories such as ECM (extracellular matrix), endothelium and signaling (*Figure 9E*).

Discussion

This work compared the structure and diversity of gut microbiome communities of horses with and without OA and correlated bacterial community assemblages to differential gene expression of SF cells obtained from joints of horses within each group. Key findings of this study were that the fecal microbiome differed at multiple taxonomic levels in horses with naturally occurring OA disease processes compared to those without OA. Notably, horses identified as having OA in this case population were significantly older and had higher body condition scores than healthy horses, indicating further studies exploring the interaction of age and obesity in the gut-joint-axis are warranted. Furthermore, the presence of specific microbiota taxa in feces correlated to differential gene expression within SF cells in OA versus healthy horses, including those related to cell structure and innate immunity. These findings present opportunities for future avenues of treatments directed towards microbial dysregulation and systemic inflammation versus the joint-centric approaches that have been historically employed in the treatment of OA, with translational relevance across species.

Preceding studies in the equine model have supported the importance of microbiota to maintenance of health and explored the association of microbiome dysregulation in disease processes other than OA (42). Differences in the microbiome of horses have been demonstrated in specific disease states such as colic, laminitis, gastric ulceration, equine recurrent uveitis, trigeminal mediated headshaking, equine grass sickness (38,43-47) and as the result of individual, treatment and management factors including signalment, sex, diet, body condition, geographic location, season, and administration of antibiotics and gastroprotectants (37,48-55). Microbial community structures have further been shown to vary between sampling locations within the hindgut of horses (54). Interestingly, network analyses of correlations between body condition, blood analytes and microbial composition at the genus level within feces revealed that specific bacterial species and assemblages may be signatures of obesity versus leanness in horses, representing a first step towards targeted strategies for microbial intervention (55). Roth *et al.* built on this to further compare the inflammatory response of macrophages exposed to fecal extracts from obese (BCS ≥7/9) versus lean BCS (4–5/9) horses and demonstrated that fecal extracts from obese individuals presented higher concentrations of lipopolysaccharide (LPS) and induced increased expression of pro-inflammatory cytokines interleukin-1B (IL-1β), tumor necrosis factor-a (TNF-α), and interleukin-6 (IL-6) from macrophages (56). These findings suggest important differences in enteric microbial composition of lean versus obese horses and demonstrate a role for the microbiome in mediating the inflammatory response, which may be highly relevant to propagation of multiple disease states, including OA.

Building support for the concept that systemic inflammation drives inflammation at distant sites (i.e., joints), prior work in horses has further shown that inflammation seen in OA is systemic and not strictly isolated to the affected joint. In experimentally induced carpal OA, differential regulation of specific genes (*ADAMDEC1*, *GRP94*, *HCST*, *bUNC-93A*, *RRM2*) in peripheral leukocytes of horses following OA induction was shown (57). In addition, remote site as well as local treatment effects following intra-synovial corticosteroid injection with triamcinolone with respect to articular cartilage glycosaminoglycan content were seen, further suggesting that downstream OA effects and treatments applied are not limited to the joint involved; however, the impact on the microbiome of native tissues has not been explored until now (58). These authors previously discussed that the link between expression of specific genes and OA was more intuitive for some compared to others, which was attributed to an incomplete knowledge of the systemic effects of OA and the intercellular signaling cascade that promotes disease progression (57). Furthermore, this study concluded that future work should be conducted to examine the gene expression profile in horses with naturally developing OA which will likely yield a greater degree of variability due to duration and severity of disease compared to the experimental model used in that study (57).

Therefore, the work described here built upon the previous body to literature to correlate microbiome dysregulation in OA to transcriptomic analyses of SF cells from joints of the same horses, which were identified to have naturally occurring progressive OA based on stringent inclusion criteria including arthroscopic evidence

of cartilage damage. Transcriptomic analyses revealed marked differential gene expression in SF cells (810 genes upregulated, 352 genes downregulated in OA) while pathway analysis revealed upregulation of inflammatory responses, eicosanoid and complement pathways in OA. Specific bacterial phyla (*Firmicutes*, *Verrucomicrobia*, *and proteobacteria*), correlated to these transcriptomic differences, generally related to either cell structure, extracellular matrix, collagen, laminin, migration, and motility, or to the immune response to inflammation, with the *Firmicutes* phyla being overrepresented as most frequently associated to up- and down-regulated transcriptomic pathways in OA. The correlation of microbial dysregulation to transcriptomic findings was particularly interesting in the context of the human and rodent literature available related to OA (7,22). While there is limited information to support whether an overabundance of a particular bacterial strain can trigger disease processes in OA or predict an increased risk for disease development, several trends have been noted in taxa reported as associated with OA status (16). Specifically, increased *Clostridium* genus (59-63), *Streptococcus* genus (64-68), and *Firmicutes* phylum, particularly abnormally elevated *Firmicutes/Bacteroidetes* (F/B) ratios (63,69-73), have been repeatedly linked to OA, indicating similarities in microbial dysregulation in OA across species, which warrants further investigation. Interestingly, a recent paper (55) examining microbiome differences in lean versus obese horses identified similar trends, with a higher relative abundance of *Firmicutes* and lower numbers of *Bacteroidetes* and *Actinobacteria* in obese horses, suggesting some of the alterations seen in microbiome of the OA case population reported here may be the result of increased body mass rather than OA status alone, and indicating that further evaluation of the interplay between body condition, microbiome dysregulation and OA progression is indicated in horses. Therefore, an important future direction of this work will be to further investigate transcriptomic and metabolic signatures of dominant bacterial species potentially impacting the host immune system function and overall physiology of the horse.

Analyses of differential gene and pathway expression in OA cases identified several unique potential therapeutic targets that, when dysregulated, have been implicated in other disease processes but not, to the authors' knowledge, in OA. One of the most upregulated genes in SF cells of OA horses, eukaryotic translation initiation factor 4E, plays a vital role in translation initiation, the rate limiting step in protein synthesis, and has been implicated in aberrant function of the nervous system (74). A-kinase anchoring proteins (AKAPs) are essential enzymes in the cAMP signaling cascade and their dysregulation has been associated with pathophysiological conditions in the cardiovascular system including atherosclerosis and heart failure (75).

In addition, induction of expression and regulation of human beta-defensins, which were upregulated in OA horses in this study, have been implicated in osteoarthritic cartilage which suggests a role in the pathogenesis of OA conserved across species (76) and warrants further investigation in horses. Multiple homeobox genes with roles in transcription were upregulated in OA processes, specifically HOXD10, which has previously been implicated in human fibroblast-like synoviocyte migration in rheumatoid arthritis (77) were upregulated in synovial cells in OA horses, indicating a potential functional role in disease progression. Overall pathways implicated in OA here including AMP-activated protein kinase (AMOK) and mechanistic target of rapamycin (mTOR) have further been previously associated with metabolism in chondrocyte dysfunction and OA progression (78). Several themes arose when evaluating differences overall, including dysfunction of intercellular signaling, innate immune cell chemotaxis, and neurodegenerative processes which may represent future therapeutic pathways. When evaluating pathways upregulated both systemically (in PBMC) and locally (in synovial cells) of horses with OA, pathways related to cell communication, response to stimuli and movement of cellular or subcellular components, vesicle mediated transport, and actin-filament and microtubule-based processes were some of the most upregulated. When evaluated overall pathways downregulated in both cell types, metabolic, cellular, and immune system processes as well as response to stimuli and biological regulation were significantly suppressed in horses with OA.

Finally, the significant upregulation of serotonin receptor 5-HTR2A in synovial cells of OA horses warrants further discussion in the context of future therapeutic targets in OA. Humans with clinical depression and suicidal ideation have been reported to have higher concentrations of serotonin receptors than healthy patients, suggesting that post-synaptic receptor density is involved in the pathogenesis of depression (79). Furthermore, physician-diagnosed depression has been reported in up to 60% of human patients with OA, a much higher rate than that of the population overall, presumably due to loss of function and associated comorbidities (80). When the presented here

data were interrogated further specifically for serotonin-related pathways and differential gene expression, serotonin receptor 467 and NR3C signaling pathway was significantly upregulated ($P<0.05$) with two additional significantly upregulated DEGs related to serotonin receptor function: GNAS complex locus and serotonin receptor HTR7 5-hydroxytryptamine receptor 7. A previous *in vitro* study using equine chondrocytes from osteoarthritic equine joints implicated neurotransmitter 5-HT and opioid receptors in OA as chondrocytes in different inflammatory stages reacted differently to 5-HT with respect to intracellular Ca^{2+} release and expression of peripheral pain mediators (81). As our findings represent the first instance of objective detection of upregulation of serotonin receptors in horses with OA to the authors' knowledge, which has been associated with depression in humans, these findings suggest that further investigation of serotonin antagonism as a multimodal approach to OA in horses may be indicated. Serotonin receptor antagonists and reuptake inhibitors such as trazadone are available in equine practice and have been recently described in the context to treat other musculoskeletal disorders in horses such as laminitis (82), although further investigation of more selective serotonin reuptake inhibitors (SSRIs) to treat OA represents a potential future direction of this work. Forthcoming studies integrating multi-omic analyses may shed further light on the pathogenesis of pain in OA and lack of congruency between radiographic findings of OA and clinical lameness or pain detected on examination in individual cases, which represents a future direction of this work.

Of note, multiple cytokines that were differentially expressed in the SF and plasma of OA and healthy horses have been previously implicated to play a role or have prognostic value in assessing the severity of OA. Six cytokines were found to be upregulated in SF of OA horses including IL-1β, IL-6, G-CSF, IP-10, IL-17A, and IL-18. IL-1β is well-recognized as one of the primary pro-inflammatory cytokines involved in OA pathogenesis, inducing cartilage degradation, reducing cartilage extracellular matrix, and inhibiting collagen synthesis (83-85). The roles of these cytokines in OA progression have been comprehensively reviewed elsewhere (83) with specific examples mentioned here. For example, both IL-6 and IP-10 have been associated with increased pain in human hip OA and were detected at greater levels in SF (IL-6 and IP-10) and synovium (IP-10) in human OA patients (86). Granulocyte colony-stimulating factor (G-CSF) regulates granulocyte lineage development and plays a role in inflammation, and G-CSF receptor blockade has been shown to ameliorate arthritis pain and disease progression (87). A role for IL-17A in OA pathophysiology has been described as IL-17 is found at higher levels in OA joints in people and noted to induce gene expression associated with experimental OA, human knee OA and other musculoskeletal disease gene-sets (88). Finally, IL-18, an IFN-γ inducing factor, has been described to be elevated in human knee OA patients and to correlate strongly with matrix metalloproteinase (MMP)-3 in people (89). In addition to some of the above cytokines, IL-2 and IFN-γ were additionally elevated in plasma of OA horses in this study cohort. Interleukin-2 is an essential cytokine for T-regulatory cell function and can further inhibit Th17 cell proliferation (90). IL-2 directed therapies have been investigated in the treatment of rheumatoid arthritis and may warrant further evaluation in the context of OA. Interestingly, IL-6 and IL-2 were upregulated in PBMC of OA horses, which correlated well to elevated cytokine levels detected via multiplex immunoassay.

The findings of this work build further support to investigate strategies to manipulate the gut microbiome have to mitigate joint degeneration. Interestingly, greater concordance in the literature actually exists to support administration of specific bacteria strains to alleviate OA symptoms (e.g., *Streptococcus thermophilus*, *Bifidobacterium longum*, *Lactobacillus casei*) rather than to distinguish OA from healthy controls (16). Obesity has been associated with loss of beneficial *Bifidobacteria* while other pro-inflammatory species gain in abundance (7). These findings highlight the complexity of the role of microbiota, even within a specific genus (e.g., *Streptococcus*), to perpetuate joint disease. Administration of prebiotic fibers such as oligofructose has been shown to restore a lean gut microbial profile, suggesting this may be a novel approach to management of obesity-associated OA (7). Furthermore, a decrease in butyrate-producing bacteria is known to be associated with obesity and metabolic disorders, and more recently with multiple orthopedic conditions, which has been postulated to be due to limited physical activity in those situations and further supports metabolite supplementation as a potential therapeutic avenue (91). Antibiotic use has been historically cited to adversely affect microbial diversity, potentially leading to dysbiosis and translocation of bacteria themselves, or their metabolites and toxins as a result of increased gut permeability (92). However, multiple studies support a therapeutic benefit for specific antibiotics (e.g., tetracyclines, macrolides, chloramphenicol, rapamycin,

penicillins, aminoglycosides) to mitigate OA disease progression (71,93-97). These findings are concordant with a body of literature utilizing preclinical models of other musculoskeletal conditions (e.g., osteoporosis, maintenance of muscle mass, and orthopedic surgical procedures), where microbiome regulation has been associated with positive outcomes (98).

Furthermore, evidence suggests that dietary supplementation with joint-protective neutraceuticals such as glucosamine, chondroitin, and type 2 collagen (UT2C) reduce symptoms associated with OA, which could be related to a gut microbial role in disease progression (7,22). For example, mice fed UT2C, or glucosamine demonstrated improvement in markers of joint health evidenced by increased uncalcified cartilage and Safranin O+ chondrocytes compared to vehicle controls, which was mirrored by global changes in the microbiome including phyla alterations with an increased *Bacteroidetes/Firmicutes* ratio in treated mice (22). Efficacy of neutraceuticals has been historically difficult to define using available biological measures, but these recent studies suggest they exert a beneficial action on joint health through modulation of the gut microbiome, although causal proof requires additional study. Finally, reducing adiposity with the goal of minimizing systemic inflammation in OA warrants further investigation related to alteration of the gut microbiome. The impact of weight loss on lameness associated with hip OA has been previously evaluated in Labrador Retriever dogs (8). A weight-loss protocol that involved feeding a high protein low-fat diet for 90 days resulted in reduced body condition and lameness scores as well as improvement in other markers of systemic inflammation including decreased mean relative neutrophil counts, serum cholesterol, calcium, and C-reactive protein (8). Although alteration of the gut microbiome was not evaluated in this study as the source of inflammation, these findings further support the benefits of weight loss as part of a multimodal treatment plan for OA. In summary, future studies will investigate modulation of microbiome niches with therapeutic interventions to correct microbial shifts that induce inflammation and subsequent degeneration in diarthrodial joints.

Several limitations to study design warrant further discussion. A primary goal of this work was to use next-generation sequencing approaches to interrogate the microbiome and transcriptome to demonstrate functional differences in feces, SF and PBMC in healthy horses compared to those with naturally occurring OA disease processes. These analyses provide a more comprehensive understanding of pathways affected during natural degenerative joint disease progression which may be relevant towards identification of specific genes in modulation of OA progression. These initial findings represent a platform from which future studies will build, towards elucidating molecular mechanisms of pathophysiology and identifying novel therapeutic targets in OA tailored to individuals in terms of body mass index, stage of disease, and OA subset such as synovitis versus post-traumatic conditions. This study is limited in terms of the small number of biological replicates, which further precluded evaluating sex differences or comparisons between transcriptomes of cells isolated from different joints (e.g., carpus *vs.* tarsus). While the sample size reported here was sufficient to detect differences in microbiome and inflammasome and correlations to OA specifically (unrelated to age or body mass), there was significant overlap in microbial species associated with OA and elevated body condition score and age concurrently. Additionally, an alternative interpretation of the elevation in inflammatory cytokines seen in plasma of OA cases may represent age-associated 'inflammaging' differences rather than a true alteration due to OA alone. Finally, while horses enrolled had been administered a consistent diet for a minimum of two months prior to sample collection, it is unclear from mouse studies and, to the authors' knowledge, unknown in horses how plastic the gut microbiome is (i.e., how long it would take for dietary changes to have a strong effect on the gut microbiome), which represents an additional limitation. Further enrollment of cases is necessary to fully account for variables such as body mass index, age, diet, and sex by OA diagnosis. Analyses were performed using samples from horses with naturally occurring OA and it is recognized that this small sample size is unlikely to be representative of the heterogeneity of disease processes considered OA.

In addition, further transcriptomic analyses are warranted to elucidate the variability in gene expression profiles in OA patients due to individual factors including disease duration, severity and number of joints affected; however, the cases presented here are likely more representative of the clinical scenario faced by physicians treating OA compared to employing a model of experimentally induced PTOA. In this study, the identity of SF cells used for transcriptomic analyses was not determined as there was insufficient cells to perform additional biomarker evaluation (e.g., by flow cytometry). It is further acknowledged that the transcriptomes of the PBMC may have been altered by cell subtype differences; however, immunophenotyping

of these mixed cellular populations was beyond the scope of the current study. Additional cross-sectional studies encompassing multiple time points may represent the best approach to distinguish core vs transient bacterial populations in disease progression. While environmental contamination is always a concern with studies of this nature, during all steps of the analysis, measures were taken to reduce bacterial contamination including sterile preparation of all collection tools and utilization of clean and controlled laboratory environments while performing library prep and sequencing steps. Furthermore, negative controls were included from each sampling step which did not yield evidence of contaminants.

Finally, although detection of bacterial DNA in IA tissues and gut dysbiosis has been repeatedly linked to progressive OA in humans and rodent models (16,17), it is not clear if these represent live organisms, or how microorganisms are transported to the joint. Microbes or their DNA have been proposed to most likely arrive in the synovium carried within leukocytes (e.g., monocytes or neutrophils), though it is possible they circulate freely in plasma (16,17). Gut microbiota have been presumed to be the major source of microbial PAMPs such as LPS as well as pro-inflammatory cytokines (e.g., IL-1β, TNF-α, IL-6) which are proposed to initiate synovial macrophage activation in OA (18). Moreover, recent evidence suggests that microbial populations present in plasma may also contribute directly to OA progression (99). However, the nature of gut inflammation at the level of the gut exfoliome has not been incorporated in previous studies, nor have all three potential sources of microbes in the joint (i.e., gut, circulating leukocytes, joint) been interrogated concurrently to determine how closely related the populations may be. Therefore, future directions of this work will concurrently interrogate all three potential sources of microbes in the joint (i.e., gut, circulating leukocytes, joint tissues) to determine how closely related the populations may be, to distinguish core versus transient populations or subsets of populations within individual articular tissues longitudinally, and investigate the downstream systemic inflammatory signature culminating in macrophage migration to the synovium and accelerate OA. These studies will fill a critical gap in our understanding of how the dysbiotic gut and the systemic inflammatory response of obesity may drive progressive OA and further our understanding of the mechanistic underpinnings of microbiome-skeletal interactions in disease, with important translational impact to humans and other species suffering from similar disease processes.

Conclusions

The gut microbiome has a profound influence on systemic inflammation and chronic musculoskeletal disease such as OA. These findings provide compelling evidence for a link between obesity, gut microbiome dysbiosis and development of naturally occurring OA in horses, establishing a connection here to further investigate disease modifying therapies. Further analysis of causation integrating fecal microbiota transplant methods with metabolomic studies of mediators produced by microbiota and examination of their impact on host physiology to perpetuate degenerative joint disease is indicated. As currently available treatments for OA are palliative, future studies will seek to further define mechanistically the pathogenic roles of key microbial species and their interactions with innate immune cells towards disease-modifying interventions in the OA of obesity.

Acknowledgments

The authors would like to acknowledge and thank the staff of the Equine Performance Analysis Facility of the Colorado State University Orthopaedic Research Center who assisted with sample collection.
Funding: This study was funded by the USDA National Institute of Food and Agriculture Animal Health and Disease (grant No. NI22AHDRXXXG011; Project Accession No. 7003828).

Footnote

Reporting Checklist: The authors have completed the ARRIVE reporting checklist. Available at https://atm.amegroups.com/article/view/10.21037/atm-24-109/rc

Data Sharing Statement: Available at https://atm.amegroups.com/article/view/10.21037/atm-24-109/dss

Peer Review File: Available at https://atm.amegroups.com/article/view/10.21037/atm-24-109/prf

Conflicts of Interest: All authors have completed the ICMJE uniform disclosure form (available at https://atm.amegroups.com/article/view/10.21037/atm-24-109/coif). L.M.P. reports that this study was funded by the Animal

Health and Disease Grant (No. NI22AHDRXXXXG011) Project Accession No. 7003828 from the USDA National Institute of Food and Agriculture. Additional grant and contract funding sources include Grayson Jockey Club Research Foundation, NIH/NCATS CCTSI and the CSU Research Council. Current or pending patents unrelated to this work include CSU-SURF 2022-041, CSU-SURF 2021-053, CSU SURF 2023-025, and CSU STRATA 2024-016. The other authors have no conflicts of interest to declare.

Ethical Statement: The authors are accountable for all aspects of the work in ensuring that questions related to the accuracy or integrity of any part of the work are appropriately investigated and resolved. This study was approved by the Institutional Animal Care and Use Committee of Colorado State University protocol #1714 and Clinical Review Board protocol #3375, and conducted according to the national guidelines under which the institution operates and NIH Guidelines for the Care and Use of Laboratory Animals (8th edition).

References

1. Cui A, Li H, Wang D, et al. Global, regional prevalence, incidence and risk factors of knee osteoarthritis in population-based studies. EClinicalMedicine 2020;29-30:100587.
2. Yelin E, Weinstein S, King T. The burden of musculoskeletal diseases in the United States. Semin Arthritis Rheum 2016;46:259-60.
3. Shih M, Hootman JM, Kruger J, et al. Physical activity in men and women with arthritis National Health Interview Survey, 2002. Am J Prev Med 2006;30:385-93.
4. Ireland JL, Clegg PD, McGowan CM, et al. Disease prevalence in geriatric horses in the United Kingdom: veterinary clinical assessment of 200 cases. Equine Vet J 2012;44:101-6.
5. Kealy RD, Lawler DF, Ballam JM, et al. Evaluation of the effect of limited food consumption on radiographic evidence of osteoarthritis in dogs. J Am Vet Med Assoc 2000;217:1678-80.
6. Marshall WG, Hazewinkel HA, Mullen D, et al. The effect of weight loss on lameness in obese dogs with osteoarthritis. Vet Res Commun 2010;34:241-53.
7. Schott EM, Farnsworth CW, Grier A, et al. Targeting the gut microbiome to treat the osteoarthritis of obesity. JCI Insight 2018;3:e95997.
8. Verma R, Turkar S, Sethi A. Impact of weight loss on lameness associated with hip osteoarthritis in obese dogs. Explor Anim Med Res 2021;2:229-36.
9. Belshaw Z. Decision making and welfare assessment in canine osteoarthritis. PhD Thesis. University of Nottingham; 2017.
10. Pearson W, Wood K, Stanley S, et al. Exploring relationships between body condition score, body fat, activity level and inflammatory biomarkers. J Anim Physiol Anim Nutr (Berl) 2018;102:1062-8.
11. Wyse CA, McNie KA, Tannahill VJ, et al. Prevalence of obesity in riding horses in Scotland. Vet Rec 2008;162:590-1.
12. Stephenson HM, Green MJ, Freeman SL. Prevalence of obesity in a population of horses in the UK. Vet Rec 2011;168:131.
13. Johnson PJ, Wiedmeyer CE, Messer NT, et al. Medical implications of obesity in horses--lessons for human obesity. J Diabetes Sci Technol 2009;3:163-74.
14. Hamada D, Maynard R, Schott E, et al. Suppressive Effects of Insulin on Tumor Necrosis Factor-Dependent Early Osteoarthritic Changes Associated With Obesity and Type 2 Diabetes Mellitus. Arthritis Rheumatol 2016;68:1392-402.
15. Raghu H, Lepus CM, Wang Q, et al. CCL2/CCR2, but not CCL5/CCR5, mediates monocyte recruitment, inflammation and cartilage destruction in osteoarthritis. Ann Rheum Dis 2017;76:914-22.
16. Bonato A, Zenobi-Wong M, Barreto G, et al. A systematic review of microbiome composition in osteoarthritis subjects. Osteoarthritis Cartilage 2022;30:786-801.
17. Dunn CM, Jeffries MA. The Microbiome in Osteoarthritis: a Narrative Review of Recent Human and Animal Model Literature. Curr Rheumatol Rep 2022;24:139-48.
18. Huang ZY, Stabler T, Pei FX, et al. Both systemic and local lipopolysaccharide (LPS) burden are associated with knee OA severity and inflammation. Osteoarthritis Cartilage 2016;24:1769-75.

19. Creely SJ, McTernan PG, Kusminski CM, et al. Lipopolysaccharide activates an innate immune system response in human adipose tissue in obesity and type 2 diabetes. Am J Physiol Endocrinol Metab 2007;292:E740-7.
20. Cani PD, Knauf C. How gut microbes talk to organs: The role of endocrine and nervous routes. Mol Metab 2016;5:743-52.
21. Cani PD, Amar J, Iglesias MA, et al. Metabolic endotoxemia initiates obesity and insulin resistance. Diabetes 2007;56:1761-72.
22. Favazzo LJ, Hendesi H, Villani DA, et al. The gut microbiome-joint connection: implications in osteoarthritis. Curr Opin Rheumatol 2020;32:92-101.
23. Frisbie DD, Cross MW, McIlwraith CW. A comparative study of articular cartilage thickness in the stifle of animal species used in human pre-clinical studies compared to articular cartilage thickness in the human knee. Vet Comp Orthop Traumatol 2006;19:142-6.
24. McIlwraith CW, Fortier LA, Frisbie DD, et al. Equine Models of Articular Cartilage Repair. Cartilage 2011;2:317-26.
25. Chu CR, Szczodry M, Bruno S. Animal models for cartilage regeneration and repair. Tissue Eng Part B Rev 2010;16:105-15.
26. Reesink HL, Watts AE, Mohammed HO, et al. Lubricin/proteoglycan 4 increases in both experimental and naturally occurring equine osteoarthritis. Osteoarthritis Cartilage 2017;25:128-37.
27. Henneke DR, Potter GD, Kreider JL, et al. Relationship between condition score, physical measurements and body fat percentage in mares. Equine Vet J 1983;15:371-2.
28. Pezzanite LM, Chow L, Phillips J, et al. TLR-activated mesenchymal stromal cell therapy and antibiotics to treat multi-drug resistant Staphylococcal septic arthritis in an equine model. Ann Transl Med 2022;10:1157.
29. McIlwraith CW, Frisbie DD, Kawcak CE. Evaluation of intramuscularly administered sodium pentosan polysulfate for treatment of experimentally induced osteoarthritis in horses. Am J Vet Res 2012;73:628-33.
30. Frisbie DD, Kisiday JD, Kawcak CE, et al. Evaluation of adipose-derived stromal vascular fraction or bone marrow-derived mesenchymal stem cells for treatment of osteoarthritis. J Orthop Res 2009;27:1675-80.
31. Frisbie DD, Kawcak CE, Werpy NM, et al. Clinical, biochemical, and histologic effects of intra-articular administration of autologous conditioned serum in horses with experimentally induced osteoarthritis. Am J Vet Res 2007;68:290-6.
32. McIlwraith CW, Frisbie DD, Kawcak CE, et al. The OARSI histopathology initiative - recommendations for histological assessments of osteoarthritis in the horse. Osteoarthritis Cartilage 2010;18 Suppl 3:S93-105.
33. Bolyen E, Rideout JR, Dillon MR, et al. Reproducible, interactive, scalable and extensible microbiome data science using QIIME 2. Nat Biotechnol 2019;37:852-7. Erratum in: Nat Biotechnol 2019;37:1091.
34. Mandal S, Van Treuren W, White RA, et al. Analysis of composition of microbiomes: a novel method for studying microbial composition. Microb Ecol Health Dis 2015;26:27663.
35. Segata N, Izard J, Waldron L, et al. Metagenomic biomarker discovery and explanation. Genome Biol 2011;12:R60.
36. Love MI, Huber W, Anders S. Moderated estimation of fold change and dispersion for RNA-seq data with DESeq2. Genome Biol 2014;15:550.
37. Mach N, Lansade L, Bars-Cortina D, et al. Gut microbiota resilience in horse athletes following holidays out to pasture. Sci Rep 2021;11:5007.
38. Martin de Bustamante M, Gomez D, MacNicol J, et al. The Fecal Bacterial Microbiota in Horses with Equine Recurrent Uveitis. Animals (Basel) 2021;11:745.
39. R Core Team. R: A Language and environment for statistical computing. Vienna: R Foundation for statistical computing 2012.
40. Martin M. Cutadaptremovesadaptersequencesfromhigh-throughputsequencing reads. EMBnet J 2011;17:1-12. doi: 10.14806/ej.17.11.200.
41. Anders S, Pyl PT, Huber W. HTSeq—a python framework to work with high- throughput sequencing data. BioRxiv 2014. doi: 10.1101/002824.
42. Kinoshita Y, Niwa H, Uchida-Fujii E, et al. Establishment and assessment of an amplicon sequencing method targeting the 16S-ITS-23S rRNA operon for analysis of the equine gut microbiome. Sci Rep 2021;11:11884.
43. Aleman M, Sheldon SA, Jospin G, et al. Caecal microbiota in horses with trigeminal-mediated headshaking. Vet Med Sci 2022;8:1049-55.
44. McGorum BC, Chen Z, Glendinning L, et al. Equine grass sickness (a multiple systems neuropathy) is associated with alterations in the gastrointestinal mycobiome. Anim Microbiome 2021;3:70.
45. Paul LJ, Ericsson AC, Andrews FM, et al. Gastric microbiome in horses with and without equine glandular gastric disease. J Vet Intern Med 2021;35:2458-64.

46. Stewart HL, Pitta D, Indugu N, et al. Changes in the faecal bacterial microbiota during hospitalisation of horses with colic and the effect of different causes of colic. Equine Vet J 2021;53:1119-31.
47. Tuniyazi M, He J, Guo J, et al. Changes of microbial and metabolome of the equine hindgut during oligofructose-induced laminitis. BMC Vet Res 2021;17:11.
48. Arnold CE, Pilla R, Chaffin MK, et al. The effects of signalment, diet, geographic location, season, and colitis associated with antimicrobial use or Salmonella infection on the fecal microbiome of horses. J Vet Intern Med 2021;35:2437-48.
49. Cerri S, Taminiau B, de Lusancay AH, et al. Effect of oral administration of omeprazole on the microbiota of the gastric glandular mucosa and feces of healthy horses. J Vet Intern Med 2020;34:2727-37.
50. Franzan BC, Coelho IDS, de Souza MT, et al. Fecal Microbiome Responses to Sudden Diet Change in Mangalarga Marchador horses. J Equine Vet Sci 2022;108:103803.
51. Jiménez BLM, Elghandour MMMY, Adegbeye MJ, et al. Use of Antibiotics in Equines and Their Effect on Metabolic Health and Cecal Microflora Activities. J Equine Vet Sci 2021;105:103717.
52. Mshelia ES, Adamu L, Wakil Y, et al. The association between gut microbiome, sex, age and body condition scores of horses in Maiduguri and its environs. Microb Pathog 2018;118:81-6.
53. Willette JA, Pitta D, Indugu N, et al. Experimental crossover study on the effects of withholding feed for 24 h on the equine faecal bacterial microbiota in healthy mares. BMC Vet Res 2021;17:3.
54. Sorensen RJ, Drouillard JS, Douthit TL, et al. Effect of hay type on cecal and fecal microbiome and fermentation parameters in horses. J Anim Sci 2021;99:skaa407.
55. Biddle AS, Tomb JF, Fan Z. Microbiome and Blood Analyte Differences Point to Community and Metabolic Signatures in Lean and Obese Horses. Front Vet Sci 2018;5:225.
56. Roth P, Stanley J, Chamoun-Emanuelli A, et al. Fecal extract from obese horses induces an inflammatory response by murine macrophages in vitro. Am J Vet Res 2022;83:419-25.
57. Kamm JL, Frisbie DD, McIlwraith CW, et al. Gene biomarkers in peripheral white blood cells of horses with experimentally induced osteoarthritis. Am J Vet Res 2013;74:115-21.
58. Frisbie DD, Kawcak CE, Trotter GW, et al. Effects of triamcinolone acetonide on an in vivo equine osteochondral fragment exercise model. Equine Vet J 1997;29:349-59.
59. Coulson S, Butt H, Vecchio P, et al. Green-lipped mussel extract (Perna canaliculus) and glucosamine sulphate in patients with knee osteoarthritis: therapeutic efficacy and effects on gastrointestinal microbiota profiles. Inflammopharmacology 2013;21(1):79-90.
60. Lee JY, Mannaa M, Kim Y, et al. Comparative Analysis of Fecal Microbiota Composition Between Rheumatoid Arthritis and Osteoarthritis Patients. Genes (Basel) 2019;10:748.
61. Mikuls TR, Walker C, Qiu F, et al. The subgingival microbiome in patients with established rheumatoid arthritis. Rheumatology (Oxford) 2018;57:1162-72.
62. Rios JL, Bomhof MR, Reimer RA, et al. Protective effect of prebiotic and exercise intervention on knee health in a rat model of diet-induced obesity. Sci Rep 2019;9:3893.
63. Collins KH, Paul HA, Reimer RA, et al. Relationship between inflammation, the gut microbiota, and metabolic osteoarthritis development: studies in a rat model. Osteoarthritis Cartilage 2015;23:1989-98.
64. Boer CG, Radjabzadeh D, Medina-Gomez C, et al. Intestinal microbiome composition and its relation to joint pain and inflammation. Nat Commun 2019;10:4881.
65. Chen B, Zhao Y, Li S, et al. Variations in oral microbiome profiles in rheumatoid arthritis and osteoarthritis with potential biomarkers for arthritis screening. Sci Rep 2018;8:17126.
66. Ramasamy B, Magne F, Tripathy SK, et al. Association of Gut Microbiome and Vitamin D Deficiency in Knee Osteoarthritis Patients: A Pilot Study. Nutrients 2021;13:1272.
67. Moen K, Brun JG, Valen M, et al. Synovial inflammation in active rheumatoid arthritis and psoriatic arthritis facilitates trapping of a variety of oral bacterial DNAs. Clin Exp Rheumatol 2006;24:656-63.
68. Zhao Y, Chen B, Li S, et al. Detection and characterization of bacterial nucleic acids in culture-negative synovial tissue and fluid samples from rheumatoid arthritis or osteoarthritis patients. Sci Rep 2018;8:14305.
69. Chen J, Wang A, Wang Q. Dysbiosis of the gut microbiome is a risk factor for osteoarthritis in older female adults: a case control study. BMC Bioinformatics 2021;22:299.
70. Wang Z, Zhu H, Jiang Q, et al. The gut microbiome as non-invasive biomarkers for identifying overweight

people at risk for osteoarthritis. Microb Pathog 2021;157:104976.
71. Guan Z, Jia J, Zhang C, et al. Gut microbiome dysbiosis alleviates the progression of osteoarthritis in mice. Clin Sci (Lond) 2020;134:3159-74.
72. Song W, Liu Y, Dong X, et al. Lactobacillus M5 prevents osteoarthritis induced by a high-fat diet in mice. J Funct Foods 2020;72:104039.
73. Li K, Liu A, Zong W, et al. Moderate exercise ameliorates osteoarthritis by reducing lipopolysaccharides from gut microbiota in mice. Saudi J Biol Sci 2021;28:40-9.
74. Amorim IS, Lach G, Gkogkas CG. The Role of the Eukaryotic Translation Initiation Factor 4E (eIF4E) in Neuropsychiatric Disorders. Front Genet 2018;9:561.
75. Ercu M, Klussmann E. Roles of A-Kinase Anchoring Proteins and Phosphodiesterases in the Cardiovascular System. J Cardiovasc Dev Dis 2018;5:14.
76. Varoga D, Paulsen FP, Kohrs S, et al. Expression and regulation of human beta-defensin-2 in osteoarthritic cartilage. J Pathol 2006;209:166-73.
77. Luan L, Ma Y, Zhang L. HOXD10 silencing suppresses human fibroblast-like synoviocyte migration in rheumatoid arthritis via downregulation of the p38/JNK pathway. Exp Ther Med 2018;16:1621-8.
78. Zheng L, Zhang Z, Sheng P, et al. The role of metabolism in chondrocyte dysfunction and the progression of osteoarthritis. Ageing Res Rev 2021;66:101249.
79. Eison AS, Mullins UL. Regulation of central 5-HT2A receptors: a review of in vivo studies. Behav Brain Res 1996;73:177-81.
80. Kloppenburg M, Berenbaum F. Osteoarthritis year in review 2019: epidemiology and therapy. Osteoarthritis Cartilage 2020;28:242-8.
81. Skiöldebrand E, Ley C, Björklund U, et al. Serotonin-evoked cytosolic Ca(2+) release and opioid receptor expression are upregulated in articular cartilage chondrocytes from osteoarthritic joints in horses. Vet Anim Sci 2019;8:100078.
82. Hobbs K, Luethy D, Davis J, et al. The effects of orally administered trazodone on ambulation and recumbency in healthy horses. J Vet Intern Med 2023;37:1899-906.
83. Molnar V, Matisic V, Kodvanj I, et al. Cytokines and chemokines involved in osteoarthritis progression. Int J Mol Sci 2021;22:9208. doi: 10.3390/ijms22179208.
84. Wang X, Li F, Fan C, et al. Effects and relationship of ERK1 and ERK2 in interleukin-1β-induced alterations in MMP3, MMP13, type II collagen and aggrecan expression in human chondrocytes. Int J Mol Med 2011;27:583-9.
85. Hwang SG, Yu SS, Poo H, et al. c-Jun/activator protein-1 mediates interleukin-1beta-induced dedifferentiation but not cyclooxygenase-2 expression in articular chondrocytes. J Biol Chem 2005;280:29780-7.
86. Ren G, Lutz I, Railton P, et al. Serum and synovial fluid cytokine profiling in hip osteoarthritis: distinct from knee osteoarthritis and correlated with pain. BMC Musculoskelet Disord 2018;19:39.
87. Lee MC, McCubbin JA, Christensen AD, et al. G-CSF Receptor Blockade Ameliorates Arthritic Pain and Disease. J Immunol 2017;198:3565-75.
88. Mimpen JY, Baldwin MJ, Cribbs AP, et al. Interleukin-17A Causes Osteoarthritis-Like Transcriptional Changes in Human Osteoarthritis-Derived Chondrocytes and Synovial Fibroblasts In Vitro. Front Immunol 2021;12:676173.
89. Waszczykowski M, Fabiś-Strobin A, Bednarski I, et al. Serum and synovial fluid concentrations of interleukin-18 and interleukin-20 in patients with osteoarthritis of the knee and their correlation with other markers of inflammation and turnover of joint cartilage. Arch Med Sci 2022;18:448-58.
90. Zhang X, Miao M, Zhang R, et al. Efficacy and safety of low-dose interleukin-2 in combination with methotrexate in patients with active rheumatoid arthritis: a randomized, double-blind, placebo-controlled phase 2 trial. Signal Transduct Target Ther 2022;7:67.
91. Hiltzik DM, Goodwin AM, Kurapaty SS, et al. The Role of the Gut Microbiome in Orthopedic Surgery-a Narrative Review. Curr Rev Musculoskelet Med 2024;17:37-46.
92. Weiss GA, Hennet T. Mechanisms and consequences of intestinal dysbiosis. Cell Mol Life Sci 2017;74:2959-77.
93. Zhang X, Deng XH, Song Z, et al. Matrix Metalloproteinase Inhibition With Doxycycline Affects the Progression of Posttraumatic Osteoarthritis After Anterior Cruciate Ligament Rupture: Evaluation in a New Nonsurgical Murine ACL Rupture Model. Am J Sports Med 2020;48:143-52.
94. Wu X, Cai Y, Lu S, et al. Intra-articular Injection of Chloramphenicol Reduces Articular Cartilage Degeneration in a Rabbit Model of Osteoarthritis. Clin Orthop Relat Res 2019;477:2785-97.
95. da Costa BR, Nüesch E, Reichenbach S, et al. Doxycycline for osteoarthritis of the knee or hip. Cochrane Database Syst Rev 2012;11:CD007323.
96. Cao M, Yao S, Zhu X, et al. Doxycycline Promotes Graft Healing and Attenuates Posttraumatic Osteoarthritis After Anterior Cruciate Ligament Reconstruction in a Rat

Model. Am J Sports Med 2023;51:461-75.
97. Mendez ME, Murugesh DK, Sebastian A, et al. Antibiotic Treatment Prior to Injury Improves Post-Traumatic Osteoarthritis Outcomes in Mice. Int J Mol Sci 2020;21:6424.
98. Hernandez CJ. Musculoskeletal microbiology: The utility of the microbiome in orthopedics. J Orthop Res 2021;39:251-7.
99. Arbeeva L, Azcarate-Peril MA, Cui Y, et al. Association of plasma microbial composition with a leaky gut in obesity-related osteoarthritis: An exploratory study. Osteoarthr Cartil Open 2022;4:100317.

Cite this article as: Chow L, Kawahisa-Piquini G, Bass L, Hendrickson D, Patel A, Rockow M, Dow S, Pezzanite LM. Correlation of fecal microbiome dysregulation to synovial transcriptome in an equine model of obesity associated osteoarthritis. Ann Transl Med 2024;12(6):112. doi: 10.21037/atm-24-109